32013

National Library of Canada / Bibliothèque nationale du Canada

CANADIAN THESES ON MICROFICHE / THÈSES CANADIENNES SUR MICROFICHE

NAME OF AUTHOR/*NOM DE L'AUTEUR* Jong Il Lee

TITLE OF THESIS/*TITRE DE LA THÈSE* Experimental Investigation of Steamflooding Behavior in an Adiabatic Water-Saturated Core

UNIVERSITY/*UNIVERSITÉ* U of Alberta

DEGREE FOR WHICH THESIS WAS PRESENTED/ *GRADE POUR LEQUEL CETTE THÈSE FUT PRÉSENTÉE* M. Sc.

YEAR THIS DEGREE CONFERRED/*ANNÉE D'OBTENTION DE CE GRADE* 1977

NAME OF SUPERVISOR/*NOM DU DIRECTEUR DE THÈSE* Dr D. L. Flock

Permission is hereby granted to the NATIONAL LIBRARY OF CANADA to microfilm this thesis and to lend or sell copies of the film.

The author reserves other publication rights, and neither the thesis nor extensive extracts from it may be printed or otherwise reproduced without the author's written permission.

L'autorisation est, par la présente, accordée à la BIBLIOTHÈQUE NATIONALE DU CANADA de microfilmer cette thèse et de prêter ou de vendre des exemplaires du film.

L'auteur se réserve les autres droits de publication; ni la thèse ni de longs extraits de celle-ci ne doivent être imprimés ou autrement reproduits sans l'autorisation écrite de l'auteur.

DATED/*DATÉ* Feb 18/77 SIGNED/*SIGNÉ* J. I. Lee

PERMANENT ADDRESS/*RÉSIDENCE FIXE* 5228 - Varsity Drive, N.W.
Calgary, Alta
T3A 1A6

NL-91 (3-74)

National Library of Canada

Cataloguing Branch
Canadian Theses Division

Ottawa, Canada
K1A 0N4

Bibliothèque nationale du Canada

Direction du catalogage
Division des thèses canadiennes

NOTICE

The quality of this microfiche is heavily dependent upon the quality of the original thesis submitted for microfilming. Every effort has been made to ensure the highest quality of reproduction possible.

If pages are missing, contact the university which granted the degree.

Some pages may have indistinct print especially if the original pages were typed with a poor typewriter ribbon or if the university sent us a poor photocopy.

Previously copyrighted materials (journal articles, published tests, etc.) are not filmed.

Reproduction in full or in part of this film is governed by the Canadian Copyright Act, R.S.C. 1970, c. C-30. Please read the authorization forms which accompany this thesis.

THIS DISSERTATION
HAS BEEN MICROFILMED
EXACTLY AS RECEIVED

AVIS

La qualité de cette microfiche dépend grandement de la qualité de la thèse soumise au microfilmage. Nous avons tout fait pour assurer une qualité supérieure de reproduction.

S'il manque des pages, veuillez communiquer avec l'université qui a conféré le grade.

La qualité d'impression de certaines pages peut laisser à désirer, surtout si les pages originales ont été dactylographiées à l'aide d'un ruban usé ou si l'université nous a fait parvenir une photocopie de mauvaise qualité.

Les documents qui font déjà l'objet d'un droit d'auteur (articles de revue, examens publiés, etc.) ne sont pas microfilmés.

La reproduction, même partielle, de ce microfilm est soumise à la Loi canadienne sur le droit d'auteur, SRC 1970, c. C-30. Veuillez prendre connaissance des formules d'autorisation qui accompagnent cette thèse.

LA THÈSE A ÉTÉ
MICROFILMÉE TELLE QUE
NOUS L'AVONS REÇUE

NL-339 (3/77)

THE UNIVERSITY OF ALBERTA

EXPERIMENTAL INVESTIGATION OF STEAMFLOODING BEHAVIOR IN AN ADIABATIC WATER-SATURATED CORE

BY

© JONG IL LEE

A THESIS

SUBMITTED TO THE FACULTY OF GRADUATE STUDIES AND RESEARCH

IN PARTIAL FULFILMENT OF THE REQUIREMENTS FOR THE DEGREE

OF MASTER OF SCIENCE

IN

PETROLEUM ENGINEERING

DEPARTMENT OF MINERAL ENGINEERING

EDMONTON, ALBERTA

SPRING, 1977

THE UNIVERSITY OF ALBERTA

FACULTY OF GRADUATE STUDIES AND RESEARCH

The undersigned certify that they have read, and recommend to the Faculty of Graduate Studies and Research, for acceptance a thesis entitled EXPERIMENTAL INVESTIGATION OF STEAMFLOODING BEHAVIOR IN AN ADIABATIC WATER-SATURATED CORE submitted by JONG IL LEE in partial fulfilment of the requirements for the degree of Master of Science in Petroleum Engineering.

D.W. Hlock
.....
Supervisor

Kenneth Brinkley
.....

Gerald W. Sadler
.....

Date February 9, 1977

ABSTRACT

Behavior of thermal energy utilization for steam-flooding processes was observed experimentally in a water-saturated unconsolidated core. The core was a 6 in. by 6 ft. adiabatic linear circular model, with a permeability of 19 darcies and a porosity of 42%.

The variables which were studied were dip angle, injection rate, quality and pressure of steam, and the location of the injection port.

Variation of the dip angle for the study was vertical downward to 40° upward in terms of the position of the injection port. Four different qualities of injecting steam were chosen, varying between 51 and 100% steam. The rate and pressure of steam injected ranged between 0.103 and 0.385 lb/min and between 51 and 204 psia, respectively. Two locations of the injection port were selected; one at the centre of the injection plane, and the other at the bottom of the injection plane.

Gravity override was pronounced for all the runs. The shape of the steam front was dependent on the injection rate, dip angle, and location of the injection port, but was not affected significantly by the injection pressure and quality of injected steam. That is, for the horizontal flow, in the cases of higher injection rate and lower injection port, the slope of steam front was steeper; consequently the hot water zone developed for these cases was narrower than

for the cases of lower injection rate of steam and higher location of injection port.

The growth of the steam zone was a linear function of the elapsed time for a fixed injection rate at a given injection pressure, and of the quality of steam. The steam zone size was principally determined by the amount of latent heat injected, but was not significantly dependent upon the injection pressure and the quality of steam.

ACKNOWLEDGEMENTS

The author gratefully appreciates the guidance and encouragement of Dr. D.L. Flock, Professor of Petroleum Engineering, under whose supervision this investigation was conducted. Acknowledgement is also made to Mr. G.T. Walsh for the design of many parts of the apparatus.

The author's special thanks go to Mrs. B.A. Bentsen for correcting the English and bringing into focus the sometimes fuzzy writing of an engineer, and to the staff of Data Entry, Computing Services at University of Alberta for a speedy job in entry of the manuscript.

The financial supports from the Department of Mineral Engineering and the Petroleum Aid to Education Fund are hereby acknowledged.

TABLE OF CONTENTS

	Page
LIST OF TABLES	ix
LIST OF FIGURES	x
INTRODUCTION	1
APPARATUS AND METHOD OF EXPERIMENT	5
1. Description of Apparatus and Material Preparation	5
2. Procedure and Method of Experiment	15
Determination of Steam Quality at the Injection Port	16
Measurement of Injection Rate of Steam	17
Steam Quality Control	18
Longitudinal Heat Transfer Rate through Core Chamber	18
EXPERIMENTAL RESULTS AND DISCUSSION	20
1. Vertical Downward Flood (One Dimensional Flow)	20
i) Effect of Injection Rate on Growth of Steam Zone	20
ii) Effect of Injection Pressure on Growth of Steam Zone	24
iii) Effect of Injection Quality on Steam Zone Growth	28
2. Horizontal Flood (Two Dimensional Flow)	30
i) Effect of Injection Rate on Growth of Steam Zone	30
ii) Effect of Injection Pressure on Growth of Steam Zone	35
iii) Effect of Injection Quality of Steam on Temperature Distribution	35
iv) Effect of Location of Injection Port on Angle of Steam Front and Volumetric Sweep Efficiency	39

TABLE OF CONTENTS

	Page
3. Effect of Dip Angle on Steam Zone Growth and Temperature Distribution	43
Effect of Injection Rate on Temperature Distribution for the Inclined Porous Medium	54
CONCLUSION	56
RECOMMENDATIONS	58
NOMENCLATURE	59
REFERENCES	60
BIBLIOGRAPHY	61
APPENDICES	65
A. Steam Quality Calculation at Injection Port	66
B. Comparison of Various Calculation Techniques for Injection Rate of Steam	76

LIST OF TABLES

Table	Title	Page
I	Experimental Conditions of Steamflooding into Water-Saturated Core	21
II	Comparison of Experimental Conditions Performed	22
A	Comparison of Steam Quality: Measured vs. Calculated	74
B-I	Calibration Data for Heat Loss of Steam Generator	79
B-II	Calibration Data for the Pitot Tube Flow Meter	87
B-III	Comparison of Various Calculation Techniques of Injection Rate of Steam	89

LIST OF FIGURES

FIGURE	Title	Page
1	Flow Diagram of Steamflood Experiment	6
2	Dimensions of Core Chamber	8
3	Locations of Thermocouples and Pressure Transducers	9
4	Injection Rate vs. Growth of Steam Zone (One Dimensional)	23
5	Temperature Distribution Along the Centre of the Core for the One Dimensional Flow	25
6	Injection Rate vs. Fraction of Core Occupied by Steam After 62 minutes of Injection	26
7	Injection Rate vs. Production Rate for One Dimensional Flow	27
8	Injection Pressure vs. Growth of Steam Zone (One Dimensional)	29
9	Injection Steam Quality vs. Growth of Steam Zone (One Dimensional)	31
10	Injection Rate vs. Steam Zone Growth for the Centre Injection Port (Horizontal)	32
11	Injection Rate vs. Steam Zone Growth for the Low Injection Port (Horizontal)	33
12	Temperature Distribution After 15.3 lbs of Steam was Injected at Various Injection Rates	34
13	Temperature Distribution After 6.8 lbs of Saturated Steam Injection at Indicated Pressure Level	36
14	Temperature Distribution After Injection of 10 lbs of Steam at 100 psia and Indicated Steam Quality	37
15	Temperature Distribution After Injection of 8,880 Btu of Latent Heat at 100 psia and Indicated Steam Quality	38
16	Effect of Injection Rate and Location of Injection Port on Angle of Steam Front from Horizon	40

LIST OF FIGURES

FIGURE	Title	Page
17	Effect of Injection Rate and Location of Injection Port on Total Steam Requirement to Heat the Entire Core up to the Steam Temperature	42
18A	Effect of Dip Angle on Steam Zone Growth	44
18B	Effect of Dip Angle on Steam Zone Growth	45
19A	Temperature Distribution After 37 min of Steamflood into Water Saturated Core	46
19B	Temperature Distribution After 37 min of Steamflood into Water Saturated Core	47
20	Temperature Profile of 45° Down Dip Flood	49
21	Temperature Profile of Horizontal Flood	50
22	Temperature Profile of 10° Up Dip Flood	51
23	Temperature Profile of 30° Up Dip Flood	52
24	Temperature Profile of 40° Up Dip Flood	53
25	Temperature Distribution After 14.4 lbs of Steam was Injected into the 10° Up Dip Inclination at Various Injection Rates	55
A	Comparison of Steam Quality Determination	75
B-1	Heat Loss of Steam Generator to Surroundings	80
B-2	Calibration of Pitot Tube Flow Meter for Steam Flow Rate Measurement	88

INTRODUCTION

Of all the heavy oil recovery methods, steamflooding has been one of the most attractive techniques in recent years. In order to design an efficient steamflood, it is necessary to understand how the properties of the crude oil, water and reservoir vary with temperature and how these properties interact within the reservoir during steamflooding.

Accurate information concerning how reservoir and fluid properties vary with temperature, and how they interact, is directly useful not only in the design and operation of a steamflood process, but also to test theoretical approaches to improve the method of prediction. In the early stage of bitumen recovery by steamflooding in some localities, steam is injected into the water bearing zone where, after injection of steam, only water and steam exist. To optimize the utilization of injected heat in the formation, it is necessary to understand the behavior of water and steam in the porous medium during steamflooding.

The effect of dip angle on gravity override, and consequent effect on the growth of the steam zone are necessary information for proper design of the operation. It is also desirable to know the influence of the injection rate of steam, and the quality and pressure of steam to be injected for a given reservoir, to achieve the best performance.

In 1969, Baker[1] published experimental results of a heat flow study in steamflooding, with steam displacing water in a plane-radial system which consisted of productive interval sandwiched between an overburden and underburden. He ascertained that:

(1) the heat loss to overburden and substratum was a function of time, but did not depend on injection rate;

(2) a significant portion of the injected heat was contained in the hot water zone ahead of and underlying the steam zone, and the size of the hot water zone depended on injection rate; and

(3) considerable gravity override was observed.

Later he also presented the effects of injection pressure and rate on formation heating by steamflooding in the same model used in the earlier experiment.[2] Heat losses, vertical sweep efficiency, and steam zone volume were determined for steam displacing water at different rates and pressures. Once again he concluded that:

(1) heat loss to overburden and substratum, as a percentage of the total injected, is almost solely a function of time for a given reservoir;

(2) the volume of the steam zone was found to be a function of time and the dimensionless injection parameter,

$$q_i L_v / hk_f (T_s - T_i)$$; and

(3) vertical sweep efficiency depends mostly on injection rate - improving at higher rate - and has minimal dependence on pressure and time.

The effect of pressure on the thermal energy utilization was implicitly expressed in the above dimensionless injection parameter term, indicating that the

main contribution to the heating process is due to the total thermal energy injected and is not attributed to the pressure itself.

At the onset of this work, however, no experimental or theoretical information was available regarding the effect of dip angle and quality of steam injected on gravity override and steam zone growth during steamflooding processes.

For this reason, it is desirable to investigate the influence of dip angle and various injection conditions of steam on gravity override, steam zone growth and shape of steam front during steamflooding processes. It is of course impossible to obtain all the information over the wide range of these parameters of interest; however, experimental data over a selected range of these factors are still useful not only in themselves but also as supporting information for the prediction of the effect of other factors.

An adiabatic core was employed to investigate above mentioned phenomena for simplicity, since all the heat injected stays in the experimental porous medium. Even though flood patterns in most actual reservoirs are radial and non-adiabatic, after reaching steady state, the flow behavior becomes close to linear. Furthermore, the middle section of the flood is nearly adiabatic, since the surroundings are in thermal equilibrium with this central portion of the flood.

Consequently the aim of this work was:

i) to construct equipment which is suitable for the study of recovery of heavy oil by steamflooding, steam-chemical flooding, or steam-solvent flooding;

ii) to observe gravity override, steam zone growth, shape of steam front and development of hot water zone in the water-saturated core for the various dip angles, injection qualities of steam, injection rates and injection pressures, and locations of injection port; and

iii) to make qualitative analyses of the results.

APPARATUS AND METHOD OF EXPERIMENT

1. Description of Apparatus and Material Preparation

The main part of the equipment consisted of a feed pump, a steam generator, an unconsolidated core chamber, a product manifold, a down stream flow control system, and temperature and pressure recorders. The subordinate parts were a water still, a feed-water tank, a weighing scale, a calibrated Pitot tube flow meter, heat exchangers, a steam dryer, a flow rate measuring device at down stream, and a high pressure Ruska pump as a cold water, chemical, or solvent injector. The schematic flow diagram is shown in Figure 1.

Unconsolidated Core Chamber

The unconsolidated core chamber consisted of a steel pipe, 6.625 inches in outside diameter, and 71.5 inches in length. The core chamber had a 0.275-inch thick cement liner which reduced heat transfer between the inner material contained within the pipe, and the steel pipe itself. The production end cap was fabricated with 1/8-inch radial grooves to allow fluids to flow towards the central part of the production end. Additional insulation was composed of a 2-inch layer of light carbonated commercial magnesia. Four-hundred-mesh stainless steel screens were placed at both injection and production ends to keep the unconsolidated sands in the chamber from being carried away by fluid flow.

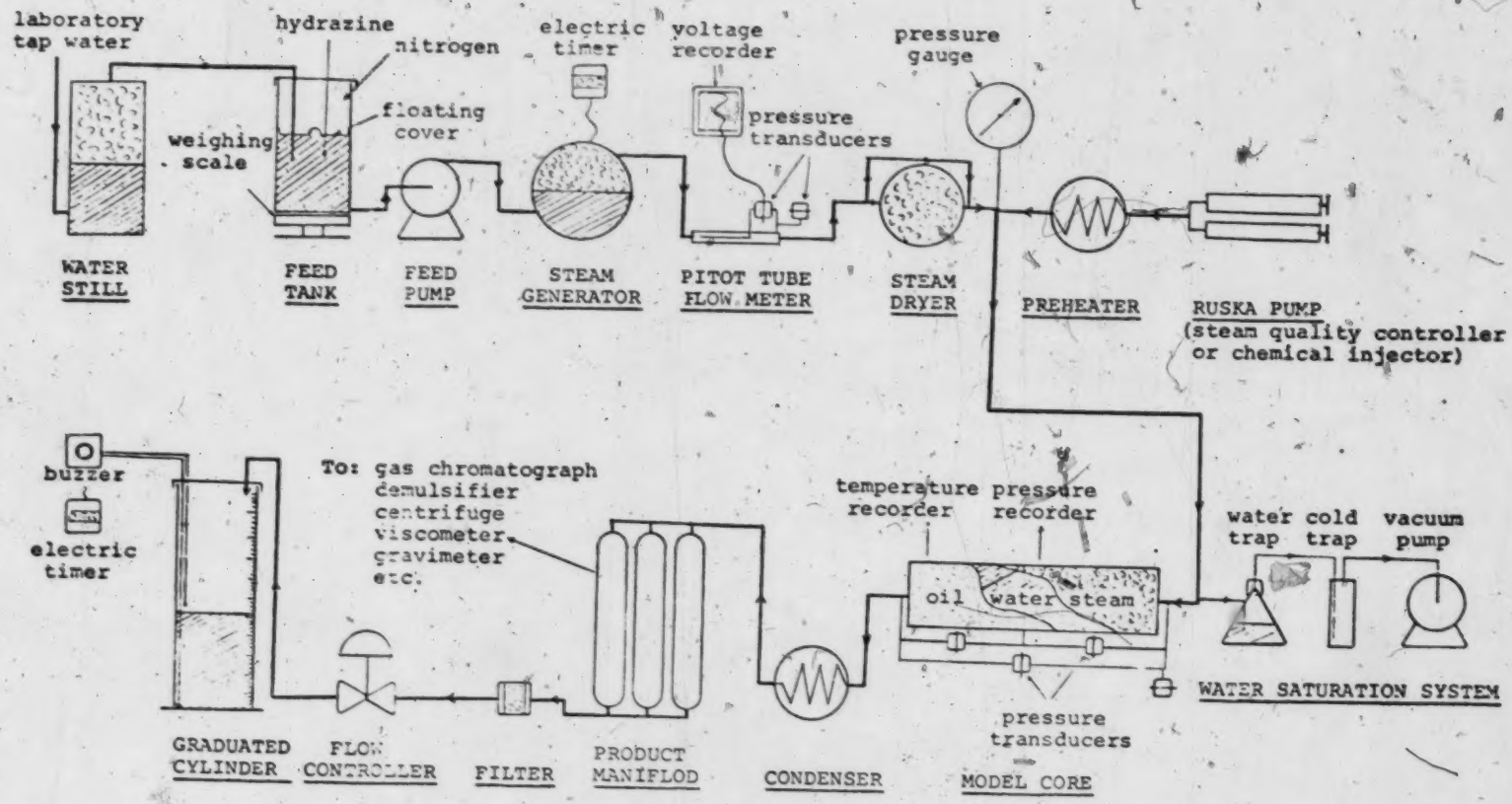

Figure 1

Flow Diagram of Steamflooding Experiment

Forty-one iron-constantan thermocouples were located along the core chamber to monitor temperature distribution at any time during the experiments. The detailed dimensions of the core chamber, and the location of the thermocouples are shown in Figures 2 and 3, respectively.

Feed Water Treatment

Laboratory tap water was boiled in a water still and the vapor was condensed to obtain mineral free distilled water which was collected into a 25-gallon feed-water tank placed on a weighing scale. To remove the dissolved oxygen from the distilled water, nitrogen was forced through from the bottom of the tank for a few minutes. To ensure the complete removal of residual oxygen and the removal of incoming oxygen from the atmosphere, hydrazine was then added in the water tank, in excess of the amount needed to remove the oxygen dissolved in the water at atmospheric pressure.

There are generally three methods of removing oxygen from process waters: by deaeration equipment, by chemical scavenging and a combination of these two methods.[3] Chemical treatments are used very often since they are simpler. They are:

catalyzed sodium sulphite,

$$Na_2SO_3 + 1/2\ O_2 \longrightarrow Na_2SO_4;$$

and hydrazine water solution,

$$N_2H_4 + O_2 \longrightarrow N_2 + 2H_2O.$$

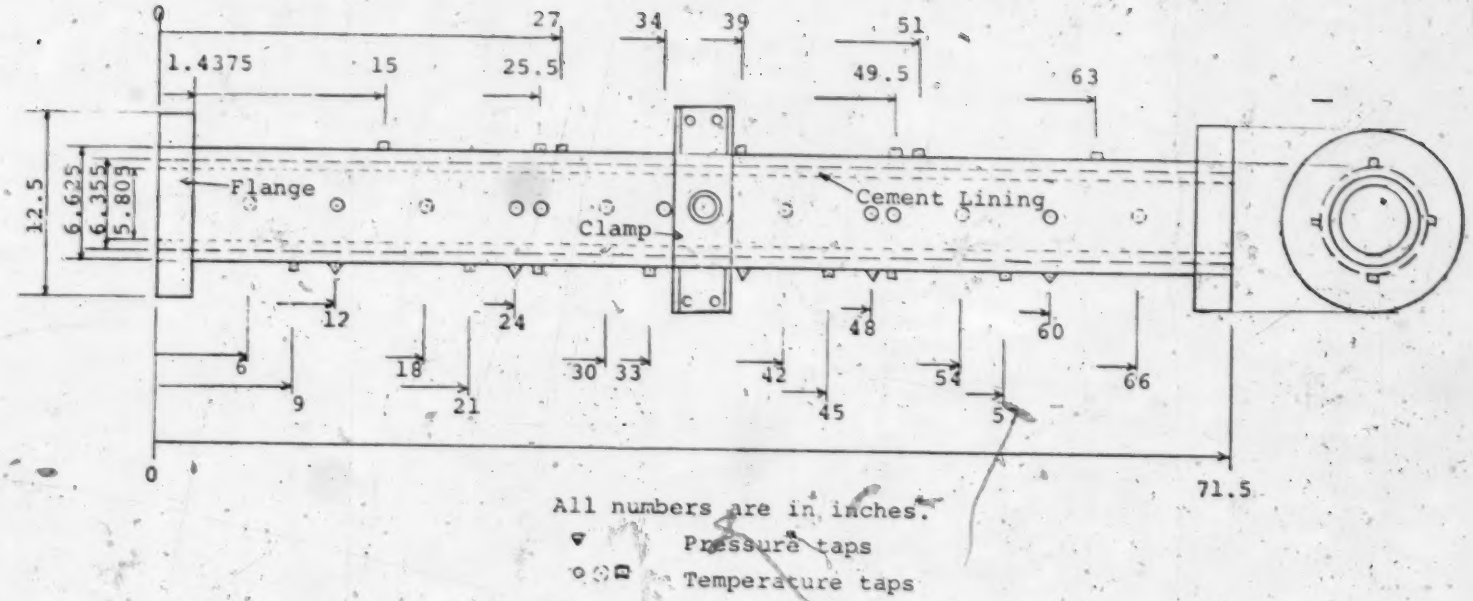

Figure 2
Dimensions of Core Chamber

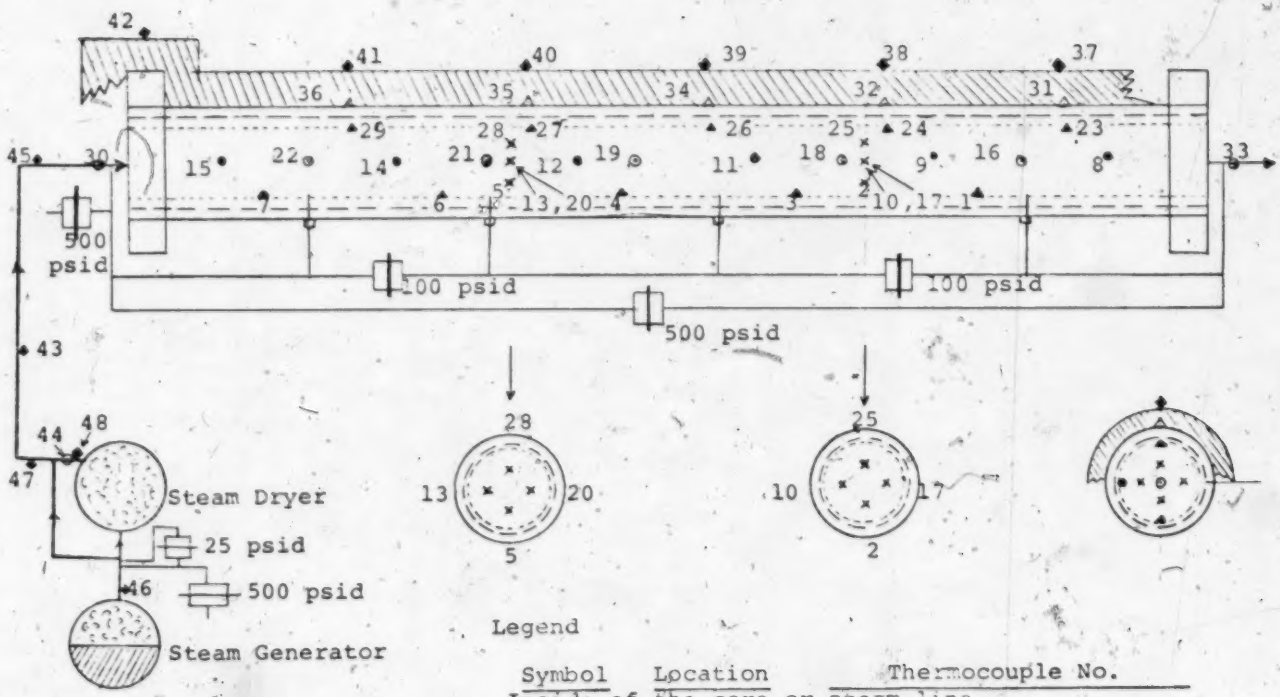

Figure 3

Locations of Thermocouples and Pressure Transducers

Legend

Symbol	Location	Thermocouple No.
Inside of the core or steam line		
○	centre	16 18 19 21 22 30 33 44
▲	top	23 24 26 27 28
▲	bottom	1 3 4 6 7
●	side	8 9 11 12 14 15
×	middle	2 5 10 13 17 20 25 28
Between the core surface and the insulation		
▲	top	31 32 34 35 36
Exterior surface of the insulation		
◆	core	38 39 40 41 42
◆	steam line	43 45 46 47 48

Even though the use of hydrazine is more costly, it was used in this experiment because it does not leave any precipitate in the treated water.

Feed Water Tank

A 25-gallon plastic container was furnished with a top lid and a floating cover, which prevents the distilled water in the feed tank from contact with the air above the water surface.

Feed Pump

To supply feed water into the steam generator a MilRoyal controlled-volume pump was installed. The pump (model A, MR7-55113 SM MilRoyal Simplex Frame A Pump) has a maximum discharge pressure of 850 psig, and a maximum discharge rate of 24 cc per second.

Steam Generator

An Ebcor steam generator (model No. 6-600-2) which has a maximum production capacity of 26 grams of 100% steam per second and is operable up to 600 psig, was used to produce steam. The generator is equipped with three electrodes which are immersed in the water of the boiler tank and was initially designed for the electrical energy input to be controlled by adjusting the water level in the tank for a fixed salinity. However, the fluctuation for a set pressure

was ±12 psi which was too high when one desired to run at a low level of pressure. For that reason it was modified so that the electric current input was controlled by an on-off switch. This modification kept the pressure variation within ±5 psi which was satisfactory for most of the experiments.

Production Manifold

Thirteen 1000-cc and ten one-gallon stainless steel samplers were connected in parallel fashion to collect products at successive time intervals. Each sampler had two ball valves at its upper and lower ends in order to isolate it from the rest of the manifold system once it was filled.

Production Rate Controller

In order to maintain a constant effluent rate of the products, a Foxboro flow rate controller was installed at the end of the manifold. The maximum allowable flow rates of this controller were 2.1 gallons per hour at 50 psid and 8 gallons per hour at 400 psid.

Injection Rate Measurement

A calibrated Pitot tube flow meter was installed directly at the outlet of the steam generator to ensure that 100 % steam passed through the flow meter. A 1/8-inch stainless steel tube of medium wall thickness was inserted concentrically into the 1/4-inch stainless steel tube line.

The differential pressure was monitored by a 25-psid pressure transducer and the resultant voltage drop due to the flow of steam was recorded on a strip chart recorder. The injection rate was indirectly controlled by regulating production rate. This was accomplished by observing the recorded output of the Pitot tube flow meter, and adjusting the flow rate accordingly.

Steam Dryer

The Pitot tube flow meter was followed by a steam dryer which generated superheated steam by heating further the steam produced from the steam generator. Steam could flow through a bypass arrangement when superheated steam was not required. The steam dryer consisted of a stainless steel coil 20 feet long, and a mercury switch which maintained a constant pressure in a little boiler containing saline water as an electrical conductor. The principle of the control was the same as the above-mentioned modified steam generator. Since the temperature of steam is a function of its saturation pressure, the setting of the pressure of the mercury switch was dependent upon the temperature of superheated steam required.

Temperature and Pressure Recorders

Two Honeywell temperature recorders, each having 24 terminals, were employed to record the temperature variation of each thermocouple by sampling each thermocouple every two

minutes. The temperature error appeared to be ± 2°F, including the thermocouple error. A Honeywell pressure recorder was used, together with a calibrated 1000-psig Heise bourdon tube gauge and six Cellesco pressure transducers, to monitor pressures at the steam generator and the injection port, as well as pressure drops across the whole core and between the inner ports.

Steam Supply Line

An 11-foot steam supply line consisted of 1/4-inch o.d. stainless steel tubing with a wall thickness of 0.035 inch. The tubing was sheathed with glass fibre pipe insulator, making the final diameter of the insulated line 2.5 inches thick. Aluminum foil surrounded the insulated line to further reduce the heat loss by radiation. Four iron-constantan thermocouples were located along the insulated steamline to measure the surface temperatures, in order that heat loss through the surface could be calculated.

Oil Sand Treatment

Sand from a well located in the Lloydminster oil field was treated by repeated soaking with toluene and steam several times until the washing fluids were clean. After this treatment it was dried at 400° F for 24 hours. It was then sieved and only the fraction between 48 and 400 mesh was used for packing in the core chamber. The sand was packed in the core chamber and compacted by air vibrators

until no further compaction was detected. It usually took about 36 hours of vibration to achieve a complete compaction. The total sand charged was 108 lbs.

Porosity and Permeability of the Core

Porosity of the core was determined by various methods: by Boyle's law (43 %); by the grain density method (40 %); by measuring weights of a fixed amount of sand, first dry and then saturated with water, and coupling this information with measurement of the final volume of the water-saturated sand after compaction in the water (38 %); and by saturating the core with distilled water (42 %). The distilled-water saturation method proceeded thus: initially the core was evacuated and distilled water was imbibed into the core, and the amount of water charged was measured. Then more water was injected into the core by a high-pressure Ruska pump to around 200 psig and the pressure drop was observed. Doing this removed the free air in the porous medium by dissolving air into the water. The distilled water was injected by the pump until no further change of pressure was observed. The distilled water injected by the pump was normally between 300 and 800 cc. This amount of water was added to the amount of water imbibed after evacuation. The total amount of water was converted into the volume which became the pore volume of the core.

Permeability was measured according to Darcy's law by flowing air or water. The resultant permeabilities obtained

by the above-mentioned two different fluids were identical, and appeared to be 19 darcies.

2. Procedure and Method of Experiment

Prior to the injection of steam the core was set at a desired dip angle. The steam generator was set at the desired pressure, with the simultaneous starting of the feed pump which was responsible for maintaining a constant level of water in the steam generator. Saturated steam passed through the steam line and bypassed to the atmosphere until the steam generator and the feed pump reached a steady-state condition.

After the stabilization of the steam feed system, the inlet valve to the core was slowly opened, and subsequently the core was pressurized to the pressure of the steam generator. Then the outlet regulating valve was set to achieve a desired effluent rate. The effluent was cooled by being passed through a condenser, and were conducted into the manifold which was initially charged with distilled water. The produced fluids purged the distilled water in the manifold by entering from the top of the sampler. The purged distilled water was collected in a calibrated measuring cylinder to indicate the total amount of effluent and to allow measurement of the flow rate of the effluent for a given time interval of interest. During the run the temperature of each thermocouple, the pressure of the steam supplied, and the pressure drops across the core and the

Pitot tube flow meter were recorded.

Determination of Steam Quality at the Injection Port

Steam quality at the injection port was determined by the equation

$$x = x_g - q_h \, l/q_i \, L_v$$

where x = the steam quality at the injection port of the core,

x_g = the steam quality at the discharge point of the steam generator (=1.0),

q_h = the heat loss rate from the steam line, Btu/hr/ft,

l = total length of the steam line, ft,

q_i = the average mass flow rate of steam, lbs/hr,

and L_v = the latent heat of the flowing steam at the average pressure of the steam generator and the injection port of the core, Btu/lb.

The heat loss to the surroundings is due to natural convection and radiation heat transfer mechanisms. The sum of these two heat transfer rates is the same as the conductive heat transfer rate through the steam line tube and its insulating sheathing. Matching these two factors with the aid of measured temperatures of steam and the temperature at the exterior surface of the insulation materials, one can estimate the heat loss rate at a given temperature of steam. The detailed method of the calculation may be obtained from Trujano, et al.[4], and is reproduced in Appendix A.

As presented in Appendix A, the calculated steam quality was in good agreement with the steam quality measured by the calorimeter. All the steam qualities presented thereafter were calculated rather than experimental.

Measurement of Injection Rate of Steam

The total mass of steam injected into the system could be measured by observing the change in weight of the water in the feed tank, or by a material balance over the total effluent, initial water amount in the core, and water required to refill the core after the run. The total amounts of produced steam calculated by the above mentioned two methods agreed within 5 %. The total amount of steam produced was divided by the total time elapsed for the run to give the average injection rate of steam. The instantaneous steam injection rate could be determined by the change of water in the feed tank for a given time interval of interest, and the accurate instantaneous steam production rate could be obtained from the measurement of the calibrated Pitot tube flow meter.

The measurement of input power rate, together with knowledge of the heat loss through the surface of the steam generator to the surroundings, gives the net electrical energy input due to the steam generation. This information, coupled with knowledge of the condition of the steam produced and total time elapsed, enabled the calculation of

the average production rate of steam, and the total steam produced.

The above-mentioned four independent methods for measuring the amount of steam generated and the average injection rate of steam were in good agreement with one another. The detailed calculation methods and comparison are presented in Appendix B.

Steam Quality Control

The steam injected might be either superheated steam, steam of various levels of quality, or hot water (zero quality steam). To generate superheated steam, the steam was passed through the steam dryer. In the case when a lower quality of steam was required, cold water at the same pressure as steam was injected at a known rate by a Ruska pump. The quality of the steam after such blending was determined by taking material and energy balances based on knowledge of the individual rates, temperatures, and pressures involved in the injection process.

Longitudinal Heat Transfer Rate through Core Chamber

The temperatures at the inner-wall of the core (Nos. 23, 24, etc., in Figure 3) were always higher in several degrees than those at the outer-wall of the core (Nos. 31, 32, etc., in Figure 3) at the same longitudinal distance from the injection port during a steamflooding process. This

indicates the fact that heat transfer through the thin pipe wall of the core chamber was not significant when compared with the convectional heat transfer in the porous medium due to the fluid flow.

EXPERIMENTAL RESULTS AND DISCUSSION

To investigate the influence of dip angle, injection rate , injection quality, injection pressure and location of injection port on the growth of the steam zone, the shape of the steam front and the development of the hot water zone, a total of fifty-one runs were conducted by injecting steam into the distilled water-saturated core. Table I summarizes the various operating conditions utilized in this work. The differences between this experiment and Baker's[1,2] works are shown in Table II.

1. Vertical Downward Flood (One Dimensional Flow)

To ensure one dimensional flow, the first eleven runs were conducted under the condition of vertical downward injection.

i) Effect of Injection Rate on the Growth of Steam Zone

Figure 4 shows the experimental results of one dimensional flow for the various injection rates ranging between 0.107 and 0.252 lb of steam per minute at around 95 psia and 99 % steam quality. The horizontal lines indicate the position of the steam front at specified times after injection.

Except for the first time interval in each run, the steam front travelled equal distances in equal time intervals. The relatively short distance

TABLE I

EXPERIMENTAL CONDITIONS OF STEAMFLOODING INTO WATER-SATURATED CORE

RUN NO.	DATE	INJ. PRESS (PSIA)	STEAM QUALITY (PERC.)	DIP* ANGLE (DEG)	INJ. RATE (LB/M)	PROD. RATE (LB/M)	TOTAL RUN TIME (MIN)	TOTAL** INJ.H2O (GAL)	TOTAL** PROD. (GAL)	DIFF.+ PRESS (PSID)	INIT. TEMP (F)	INIT. PRESS (PSIA)	INJ.x LOCATION
1	JUN 09 76	95.5	97.7	-90.0	0.1073	0.2374	172.80	2.22	4.91	2.67	72.0	30.0	CNT
2	JUN 17 76	98.7	98.7	-90.0	0.1515	0.3612	109.10	1.98	4.72	3.67	76.0	30.0	CNT
3	JUN 21 76	95.1	99.1	-90.0	0.1903	0.4852	79.00	1.80	4.59	5.33	74.0	30.0	CNT
4	JUN 23 76	88.3	99.5	-90.0	0.2520	0.6064	62.00	1.87	4.50	7.17	72.0	30.0	CNT
5	JUN 25 76	57.6	97.5	-90.0	0.1354	0.3591	102.40	1.66	4.40	4.25	70.0	30.0	CNT
6	JUN 26 76	146.6	98.9	-90.0	0.1568	0.3587	115.00	2.16	4.94	2.83	75.0	30.0	CNT
7	JUN 28 76	195.9	98.9	-90.0	0.1703	0.3601	120.60	2.46	5.20	2.28	74.0	30.0	CNT
8	JUN 29 76	98.6	58.4	-90.0	0.1939	0.3596	129.60	3.01	5.58	3.17	74.0	30.0	CNT
9	JUN 30 76	99.0	69.5	-90.0	0.1761	0.3570	122.30	2.58	5.23	3.08	76.0	30.0	CNT
10	JUL 02 76	99.4	80.0	-90.0	0.1665	0.3623	114.30	2.28	4.96	3.40	76.0	30.0	CNT
11	JUL 03 76	99.0	84.8	-90.0	0.1567	0.3601	110.80	2.08	4.78	3.17	76.0	30.0	CNT
12	JUL 05 76	96.9	98.7	0.0	0.1573	0.2350	134.30	2.53	3.78	0.00	75.0	30.0	CNT
13	JUL 06 76	90.4	99.2	0.0	0.2008	0.3599	102.30	2.46	4.41	1.30	75.0	30.0	CNT
14	JUL 07 76	96.8	99.5	0.0	0.2335	0.4862	82.60	2.31	4.81	2.00	75.0	30.0	CNT
15	JUL 08 76	98.9	99.7	0.0	0.2684	0.5133	64.40	2.07	4.73	4.30	75.0	30.0	CNT
16	JUL 09 76	49.2	98.7	0.0	0.2625	0.3596	40.40	1.27	1.74	1.30	75.0	30.0	CNT
17	JUL 10 76	149.7	100.0	0.0	0.2778	0.3594	60.40	2.01	2.60	0.70	75.0	150.0	CNT
18	JUL 11 76	208.6	99.4	0.0	0.2195	0.3607	118.30	3.11	5.11	1.90	75.0	200.0	CNT
19	JUL 23 76	100.4	98.6	0.0	0.1452	0.2359	166.60	2.88	4.68	1.43	76.0	100.0	DWN
20	JUL 24 76	98.1	99.0	0.0	0.1775	0.3573	112.50	2.39	4.81	3.32	70.0	100.0	DWN
21	JUL 25 76	104.6	99.4	0.0	0.2094	0.4842	80.50	2.02	4.67	6.53	77.0	100.0	DWN
22	JUL 26 76	101.3	99.6	0.0	0.2464	0.6086	62.00	1.83	4.52	9.13	76.0	100.0	DWN
23	JUL 27 76	56.8	98.8	0.0	0.2572	0.3578	49.00	1.51	2.10	5.25	76.0	50.0	DWN
24	JUL 28 76	150.5	100.0	0.0	0.2966	0.3570	60.80	2.16	2.60	3.48	76.0	150.0	DWN
25	JUL 29 76	105.1	99.8	10.0	0.2660	0.3556	61.50	1.96	2.62	5.95	77.0	100.0	DWN
26	JUL 30 76	110.3	98.9	10.0	0.1607	0.2324	143.30	2.76	3.99	3.08	77.0	100.0	DWN
27	JUL 31 76	111.7	99.8	10.0	0.2574	0.4825	77.50	2.39	4.48	6.20	77.0	100.0	DWN
28	AUG 01 76	114.2	100.0	10.0	0.3201	0.6081	54.50	2.09	3.97	7.42	76.0	100.0	DWN
29	AUG 02 76	120.4	99.5	5.0	0.2082	0.3568	102.20	2.55	4.37	4.23	78.0	100.0	DWN
30	AUG 03 76	122.2	99.6	-5.0	0.2173	0.3561	95.60	2.49	4.08	4.35	79.0	100.0	DWN
31	AUG 04 76	123.0	98.9	-10.0	0.1587	0.3564	109.40	2.08	4.67	5.70	76.0	100.0	DWN
32	AUG 05 76	121.2	99.0	-20.0	0.1610	0.3569	112.50	2.17	4.81	6.67	76.0	100.0	DWN
33	AUG 06 76	98.3	98.6	-30.0	0.1481	0.3562	107.10	1.90	4.57	8.57	76.0	100.0	DWN
34	AUG 07 76	100.7	98.7	-45.0	0.1498	0.3566	107.00	1.92	4.57	9.52	75.0	100.0	DWN
35	AUG 08 76	100.7	99.2	-45.0	0.1950	0.4823	77.90	1.82	4.50	11.82	76.0	100.0	DWN
36	AUG 09 76	100.8	99.2	-30.0	0.1658	0.3636	76.80	1.71	4.45	10.78	77.0	100.0	DWN
37	AUG 10 76	102.4	98.7	-5.0	0.1520	0.2295	163.60	2.98	4.50	3.43	78.0	100.0	DWN
38	AUG 11 76	100.6	98.4	5.0	0.1329	0.2309	173.90	2.77	4.81	3.65	76.0	100.0	DWN
39	AUG 12 76	101.3	98.9	20.0	0.1674	0.2299	129.60	2.60	3.57	3.48	77.0	100.0	DWN
40	AUG 13 76	100.9	98.8	30.0	0.1558	0.2044	118.40	2.21	2.90	3.15	76.0	100.0	DWN
41	AUG 14 76	102.0	98.8	40.0	0.1595	0.2018	120.40	2.30	2.91	2.97	75.0	100.0	DWN
42	AUG 15 76	100.5	100.0	0.0	0.3864	0.6596	39.10	1.81	3.09	9.38	77.0	100.0	DWN
43	AUG 16 76	101.2	99.0	0.0	0.1670	0.2171	118.40	2.37	3.08	3.43	78.0	100.0	DWN
44	AUG 17 76	99.3	99.8	0.0	0.2842	0.3689	47.30	1.61	2.09	5.72	75.0	100.0	DWN
45	AUG 18 76	100.3	50.7	0.0	0.1664	0.1890	240.70	4.80	5.45	2.58	77.0	100.0	DWN
46	AUG 19 76	100.5	64.6	0.0	0.1659	0.1425	165.60	3.71	4.28	2.87	75.0	100.0	DWN
47	AUG 20 76	102.4	78.5	0.0	0.1668	0.2071	140.60	2.81	3.49	3.07	78.0	100.0	DWN
48	AUG 21 76	100.5	97.6	0.0	0.1039	0.1311	240.10	2.99	3.77	2.63	75.0	100.0	DWN
49	AUG 22 76	50.7	97.8	0.0	0.1686	0.2197	80.20	1.62	2.11	4.73	75.0	50.0	DWN
50	AUG 23 76	152.1	99.1	0.0	0.1713	0.2045	118.40	2.43	2.90	2.88	75.0	150.0	DWN
51	AUG 24 76	203.5	98.8	0.0	0.1670	0.1944	118.50	2.37	2.76	2.70	75.0	200.0	DWN

* based on the injection port ** at room condition + averaged throughout the run

x cnt(centre injection port) dwn(low injection port)

TABLE II

Comparison of Experimental Conditions Performed

	Baker	This Work
Model description	Radial plane - horizontal 72" diameter x 4" height Overburden and underburden (27" water-saturated sand) Porosity 35 % Permeability 100 darcies	Linear circular with variation of dip angle 6" diameter x 71.5" length Adiabatic (4" commercial magnesia insulation) Porosity 42 % Permeability 19 darcies
Parameters studied	Injection rate (0.08-1.61 lb/min) Injection pressure (1-103 psig) Steam quality (100 %) Dip angle (horizontal) Injection port (perforated throughout the pay)	Injection rate (0.103-0.387 lb/min) Injection pressure (40-200 psig) Steam quality (50-100 %) Dip angle (40° up dip to 90° down dip) Location of injection port (centre and bottom of the porous medium)

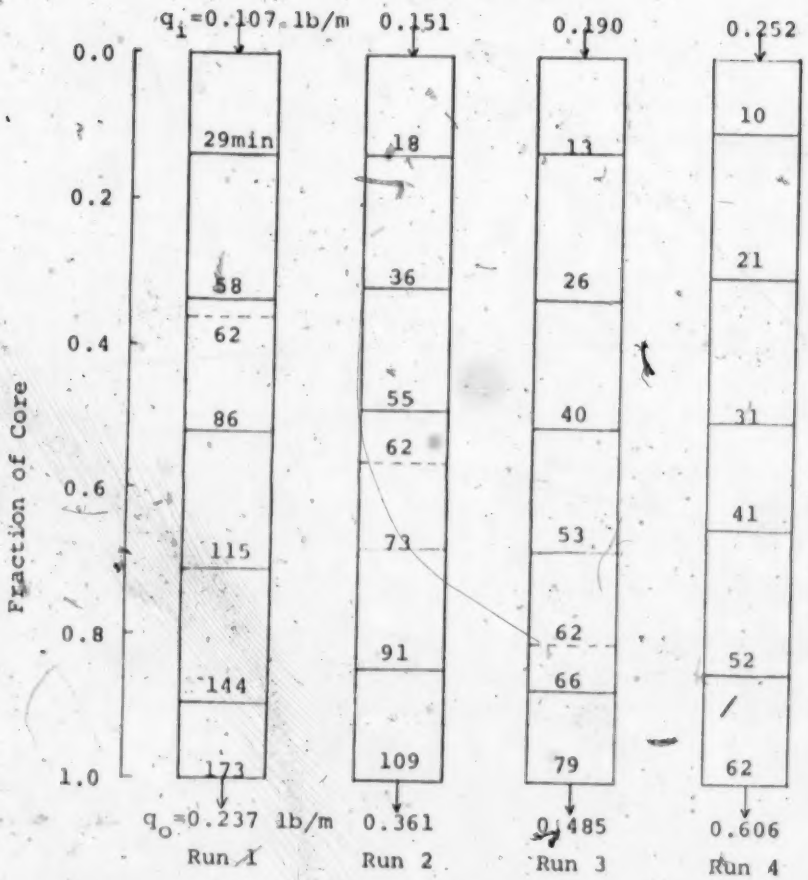

Vertical Downward Injection
Injection Pressure of Steam: 95 psia
Injecting Quality of Steam: 99 %

Figure 4

Injection Rate vs. Growth of Steam Zone (One Dimensional)

travelled during the first time period as compared to the others was due to heat lost to the flange of the core. This suggests that the steam zone growth is a linear function of the elapsed time for any injection rate when the other conditions remain constant.

Figure 5 shows the general temperature profile of typical one dimensional flow. The sharpness of the temperature profile suggests that the hot water zone developed was not significant in size.

Furthermore, as shown in Figure 6, the fraction of core occupied by steam is directly proportional to the injection rate when a fixed time interval was considered (62 minutes of injection of each run; see Figure 4). Also, a linear relationship between the injection and production rates, as shown in Figure 7, was observed at a constant injection pressure and quality of steam.

All the above results indicated that the model exhibited adiabatic behavior under all operating conditions and that the average steam quality in the steam zone was about the same.

ii) Effect of Injection Pressure on the Growth of Steam Zone

Four different pressures were selected to study the effect of injection pressure on steam zone growth,

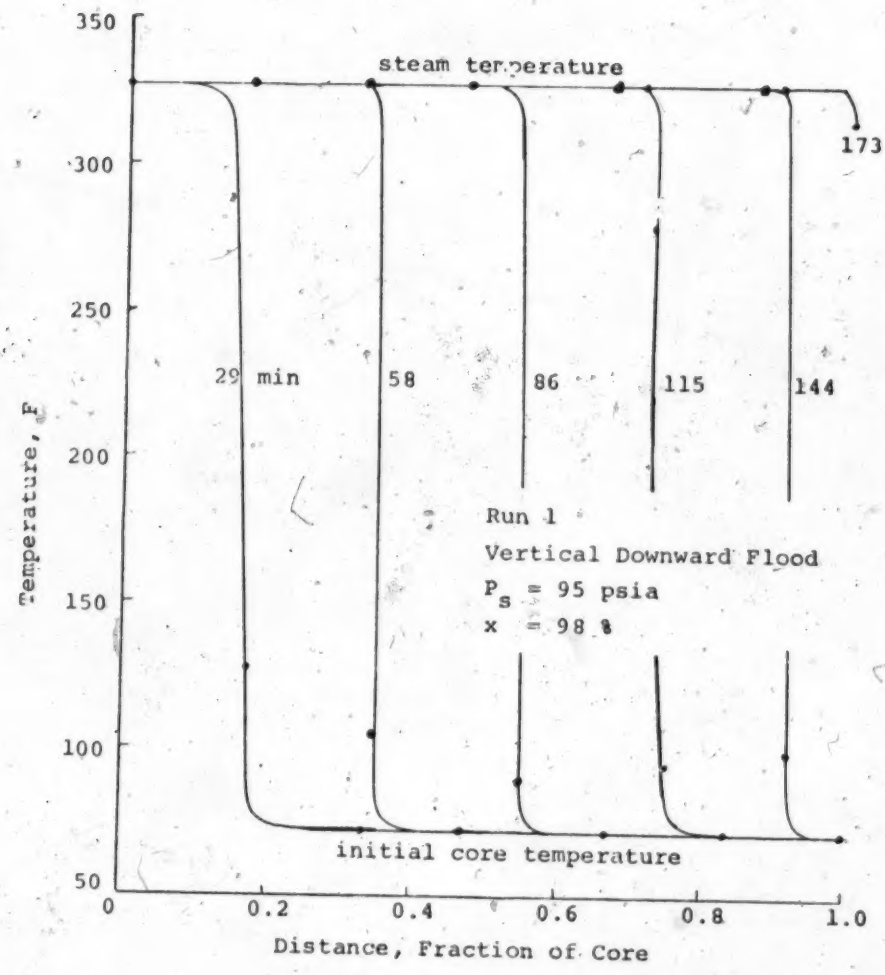

Figure 5

Temperature Distribution Along the Centre of the Core for the One Dimensional Flow

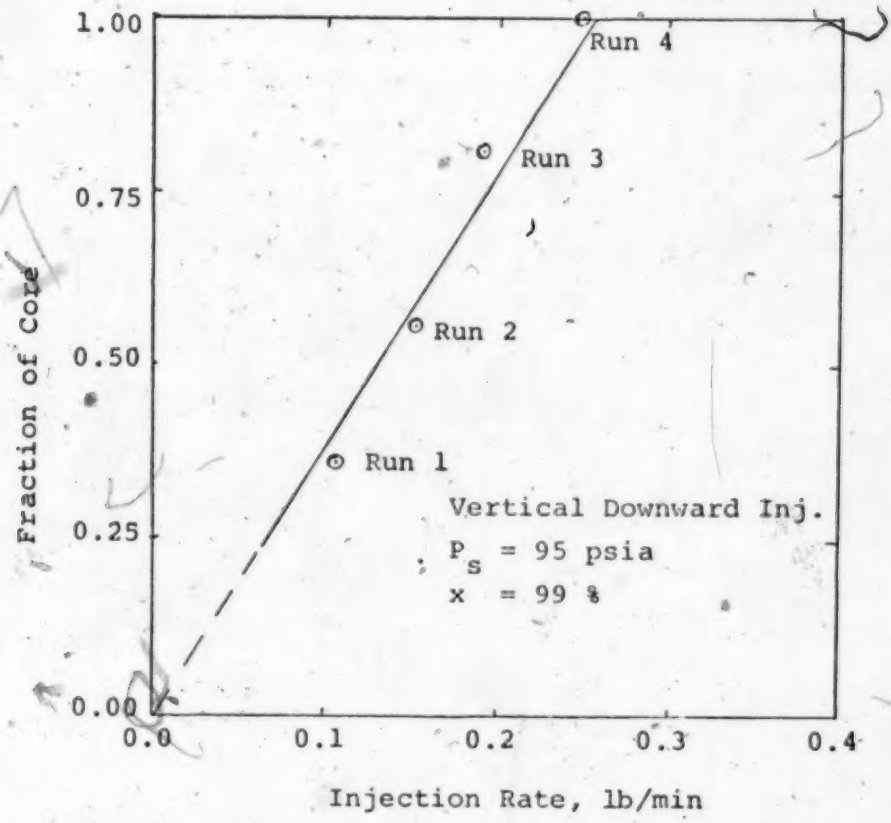

Figure 6

Injection Rate vs. Fraction of Core Occupied by Steam after 62 minutes of Injection

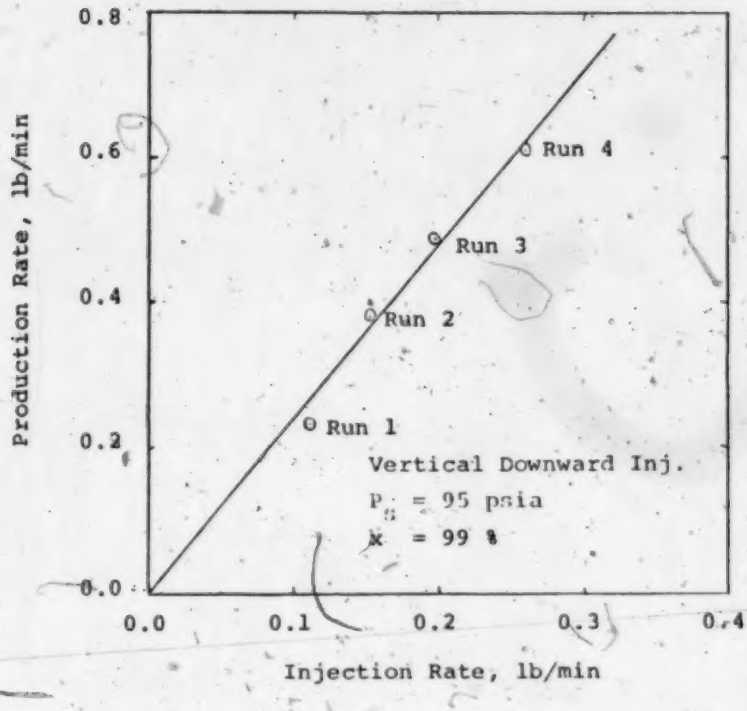

Figure 7

Injection Rate vs. Production Rate For One Dimensional Flow

i.e., at 57.6, 98.7, 146.6, and 195.6 psia. Figure 8 shows the steam zone growth with time after steam injection, for the indicated injection conditions. It may be noted from Figure 8 that, even though the injection rate and pressure were lower on some runs, the break-through time by steam was earlier than for the case of higher injection rate and pressure. However, if one compares the amount of heat utilized by steam condensation to increase the temperature by one degree, the results are same; i.e.,

$$(q_i)\,(\text{time to reach 0.5 of core length})\,(x)\,(L_v)/(T_s - T_i)$$
$$= 27.5 \pm 1.0 \text{ Btu/F (=constant)}$$

for all different pressures. This product is equivalent to the heat capacity of the first half of the core. This confirms that the model behaved adiabatically. Since at a higher steam pressure the corresponding saturation temperature is higher, therefore the temperature gradient between the core and its surroundings is greater, and the heat loss is expected to be higher, if the heat loss from the model core is significant.

iii) Effect of Injection Quality on Steam Zone Growth

Runs 8 through 11, together with Run 2, show the performances of the growth of steam zone for the different injection qualities of steam. The results are shown in Figure 9. Here again,

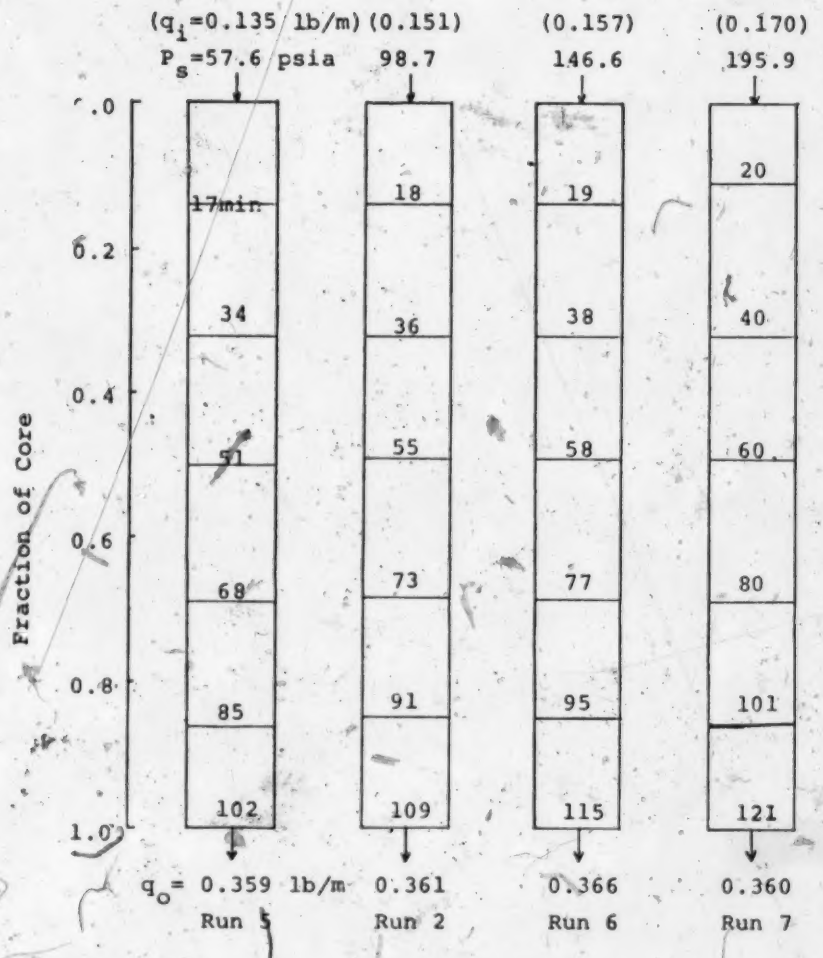

Vertical Downward Injection
Injecting Quality of Steam: 99 %

Figure 8
Injection Pressure vs. Growth of Steam Zone (One Dimensional)

(q_i) (time to reach 0.5 of core length) (x) (L_v)

= 66,500 ± 1,500 Btu (=constant)

except for the 99% steam-quality case where the product was 73,000 Btu.

In conclusion, for ideal one-dimensional flows of steamflooding processes, the size of the steam zone is determined by the total amount latent heat injected during a given time interval.

2. Horizontal Flood (Two Dimensional Flow)

Since most reservoirs are horizontal or nearly so, it is necessary to understand the behavior of horizontal flooding.

i) Effect of Injection Rate on Growth of Steam Zone

Figures 10 and 11 show the general effect of injection rate on the growth of the steam zone for the horizontal flood cases: the former for the centre injection port, the the latter for the lower injection port. As expected, as the injection rate increases, the volumetric sweep efficiency by steam improves. Figure 12 is presented to compare the temperature distribution after a constant mass of 15.3 lbs of steam had been injected under varying injection rates. Once again as the injection rate increases, the volumetric sweep efficiency tends to improve. The

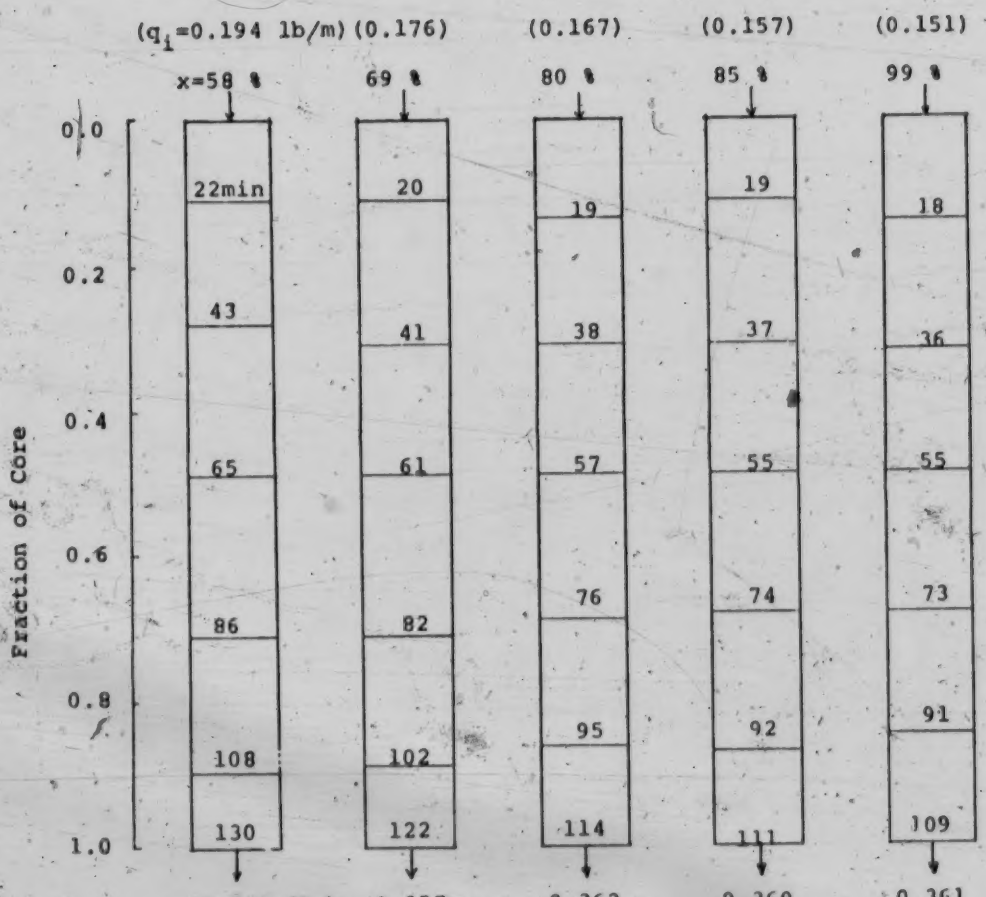

Figure 9

Injecting Steam Quality vs.Growth of Steam Zone(One Dimensional)

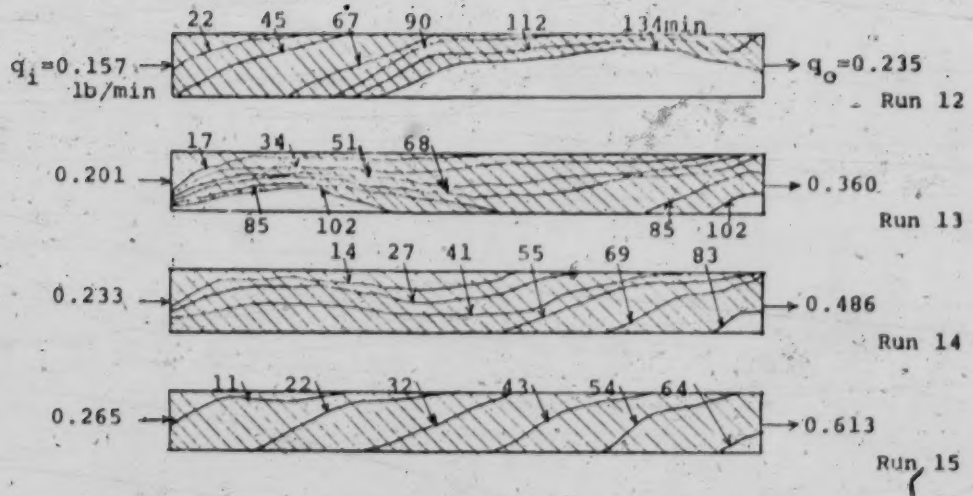

Horizontal Floods

P_s = 100 psia

x = 99 %

Figure 10

Injection Rate vs. Steam Zone Growth for the Centre Injection Port

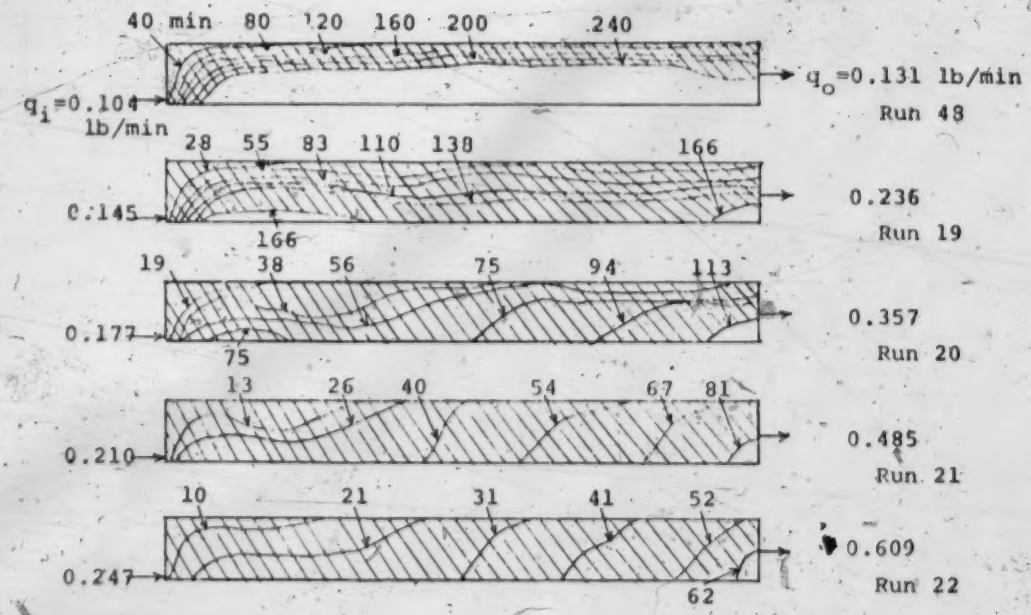

Horizontal Floods

P_s = 100 psia

x = 99 %

Figure 11

Injection Rate vs. Steam Zone Growth for the Low Injection Port

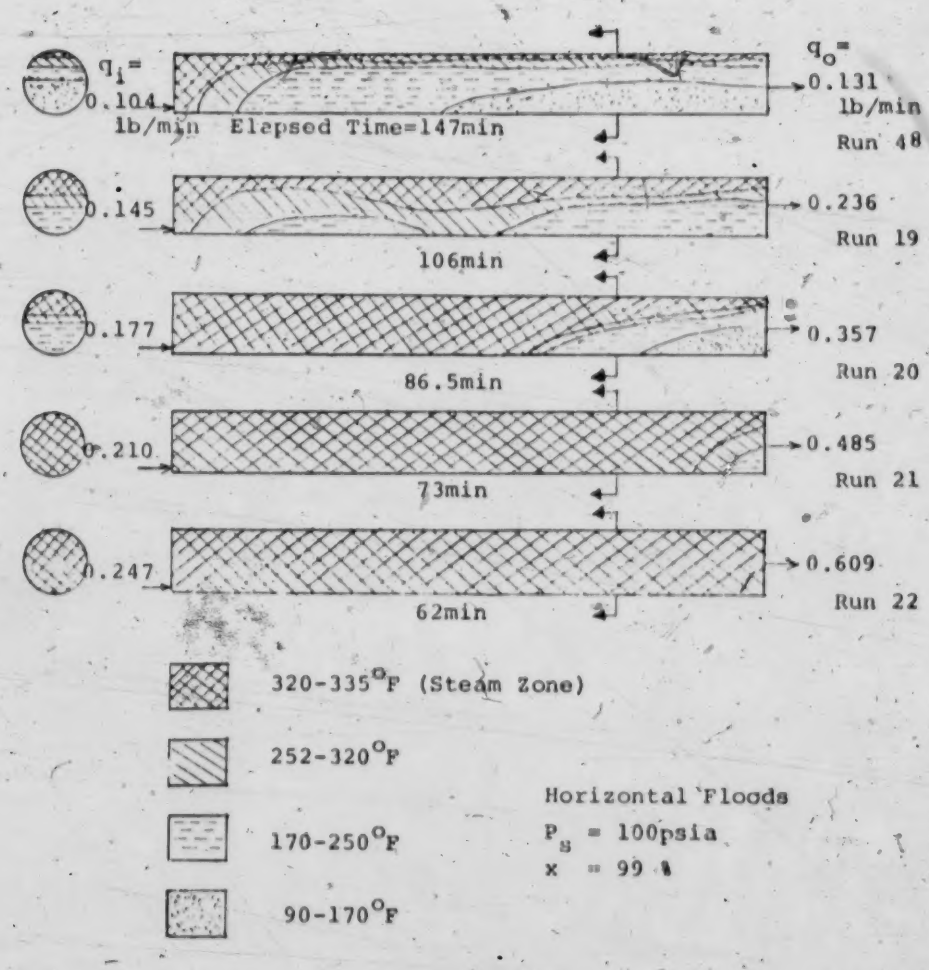

Figure 12

Temperature Distribution After 15.3 lbs of Steam was injected at Various Injection Rates

circular cross-sections illustrated in the figure show the temperature distribution across the mid-section plane of the core, normal to the direction of the injection flow.

ii) Effect of Injection Pressure on Growth of Steam Zone

The effect of the injection pressure on the over-all temperature distribution and the steam zone is illustrated in Figure 13. These results tend to support the contention that, within the pressure range studied, pressure has relatively little effect on the over-all temperature distribution and the steam zone developed during the steamflood process.

iii) Effect of Injection Quality of Steam on Temperature Distribution

Figure 14 illustrates the effect on the over-all temperature distribution of injecting 10 lbs of steam with varying steam qualities. As indicated, the over-all efficiency of the steam displacement process increases as the quality of steam increases. Figure 15 further illustrates the effect of varying the steam quality. It shows the over-all performance of the system after a total of 8,880 Btu of latent heat had been injected into the core. The results indicate that there is no significant difference in the over-all performance after injection of a fixed amount of

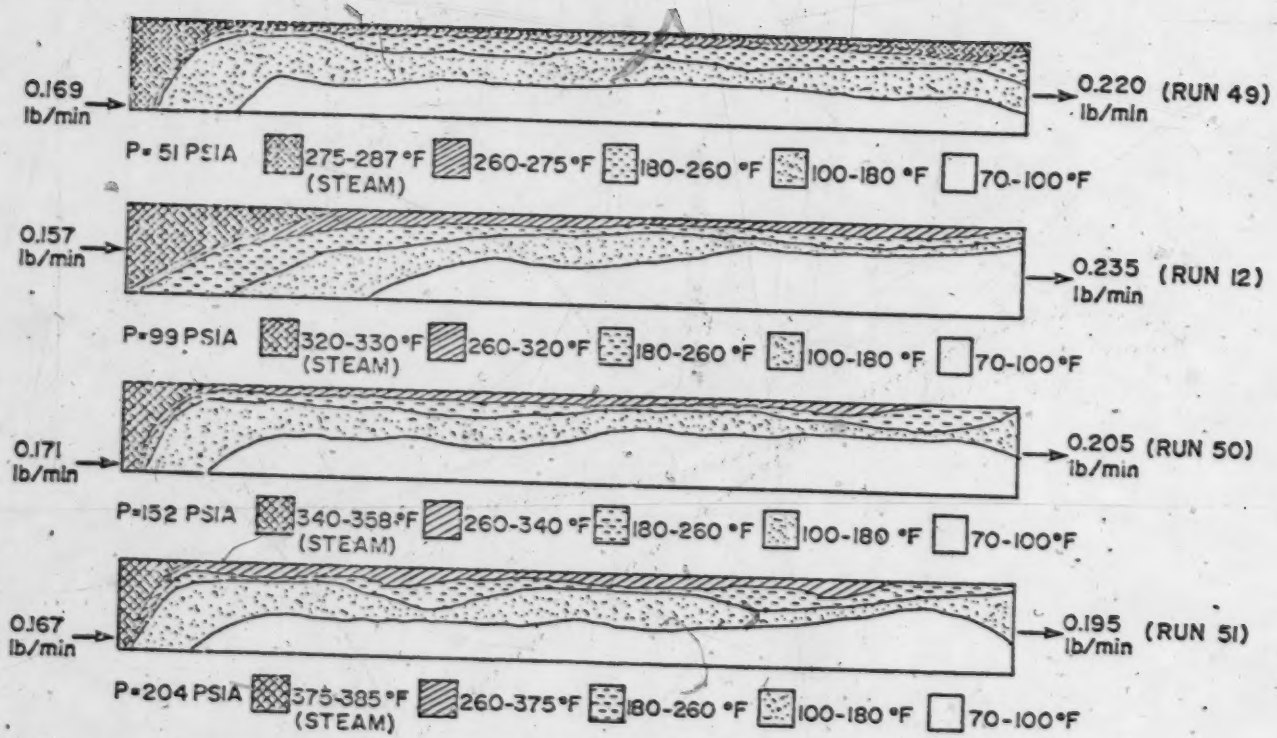

TEMPERATURE DISTRIBUTION AFTER 6.8 lb OF SATURATED STEAM INJECTION AT INDICATED PRESSURE LEVEL

— FIG 13 —

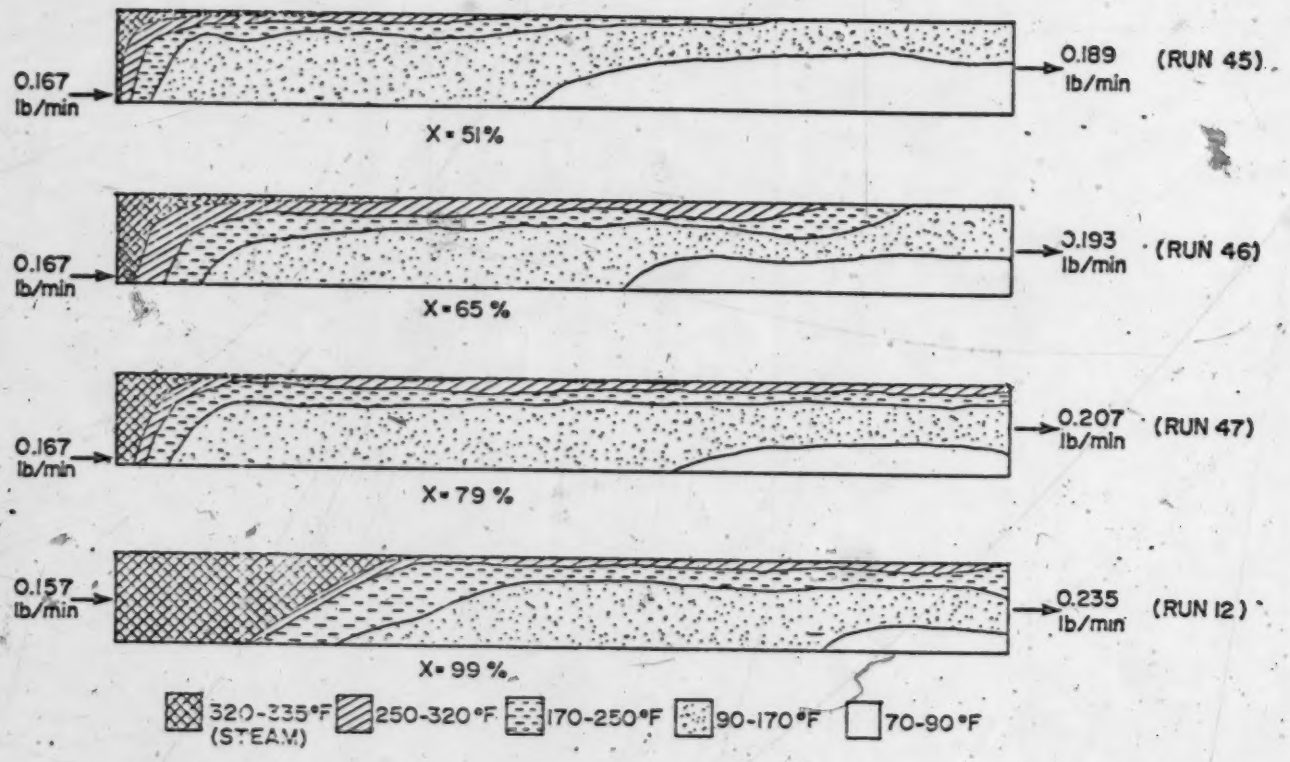

TEMPERATURE DISTRIBUTION AFTER INJECTION OF 10 lb OF STEAM AT 100 PSIA AND INDICATED STEAM QUALITY

— FIG 14 —

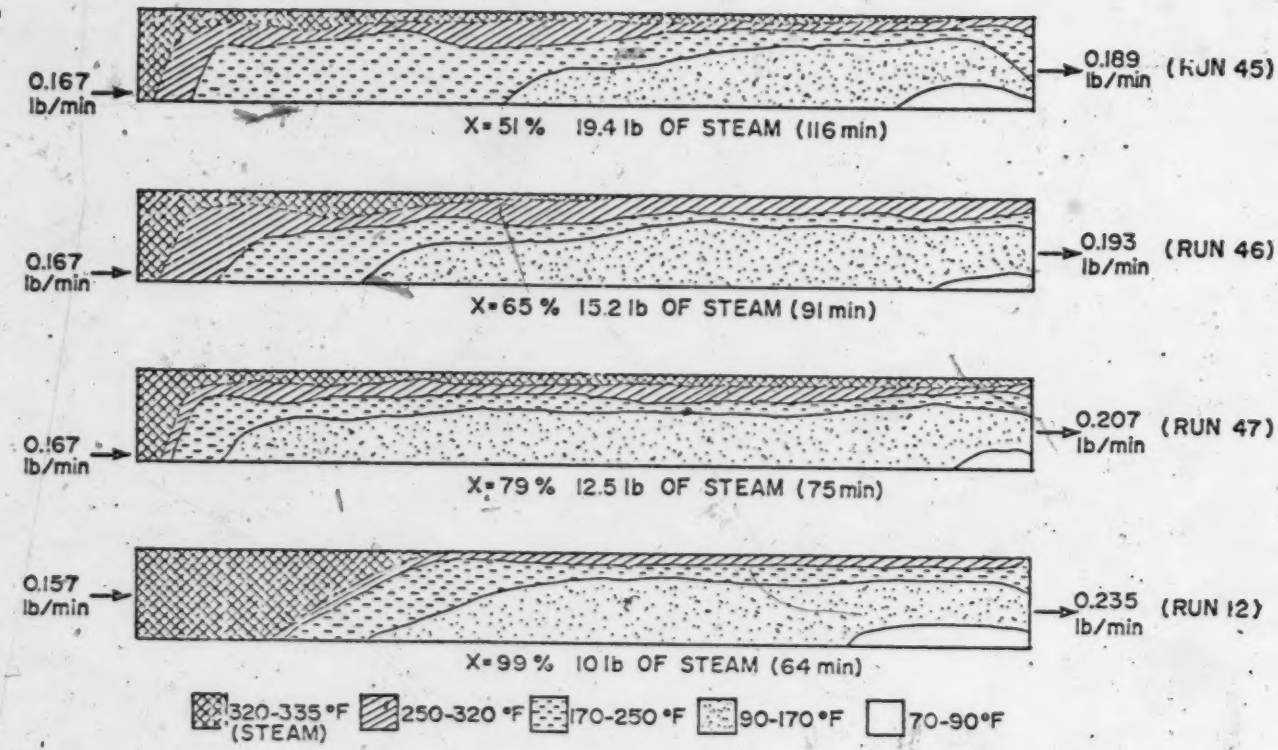

TEMPERATURE DISTRIBUTION AFTER INJECTION OF 8,880 BTU OF LATENT HEAT AT 100 PSIA AND INDICATED STEAM QUALITY

—FIG 15—

latent heat into the porous medium, regardless of differences in steam quality.

iv) Effect of Location of Injection Port on Angle of Steam Front and Volumetric Sweep Efficiency

The vertical location of the steam-injection interval affects recovery considerably. Coats[5] showed, from the results of his numerical simulator, that for a thin formation, oil recovery did not depend on the location of the injection interval. For a thick formation, however, recovery was considerably accelerated and increased as a consequence of lowering the injection port to the bottom of the interval.

Two locations of the injection port were selected to observe the effect of the port location on heat dispersion behavior during a steamflood: one at the centre of the injection plane, and the other at the bottom of the injection plane. The performances were illustrated in Figure 10 for the centre injection port and in Figure 11 for the low injection port, respectively. Figure 16 summarizes the effects of injection rate and location of the injection port on the angle of the steam front from the horizon. The angle of the steam front was measured from Figures 10 and 11. As presented in Figure 16, the angle of the steam front is always higher for the case of the bottom injection port at a constant injection rate.

Horizontal Floods

P_s = 100 psia

x = 99 %

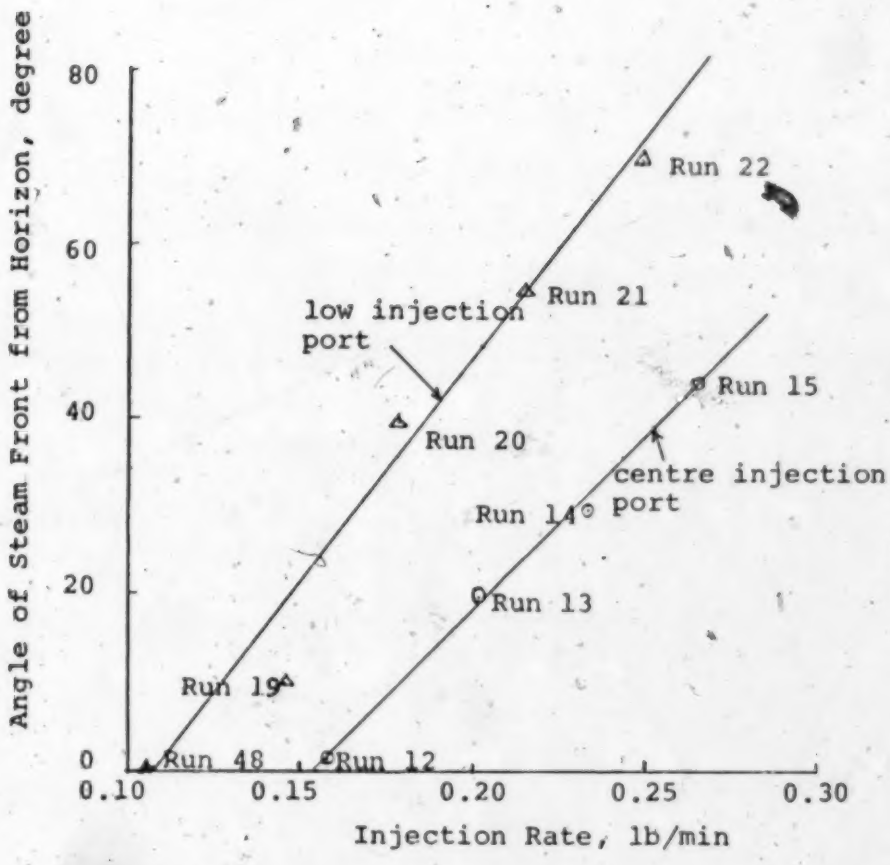

Figure 16

Effects of Injection Rate and Location of Injection Port on Angle of Steam Front from Horizon

Also, a injection rate increases, the angle of the steam front becomes steeper for both cases.

Figure 17 presents the effects of injection rate and location of the injection port on the total steam required to heat the core to steam temperature. The total steam required was obtained from Figures 10 and 11 by multiplying the rate of injection by the time to breakthrough of steam. For Runs 12 and 13 the core was not flooded by the injected steam at the time of breakthrough; rather, only 67% and 90%, respectively, of the porous medium was occupied by steam. For comparison on the same basis, the amount steam injected into the core up to steam breakthrough was divided by the fraction occupied by steam: i.e., 21 lb/0.67 for Run 12, and 20.5 lb/0.9 for Run 13. For Run 48 in Figure 11, the same procedures apply for the same reason: i.e., 25 lb/0.5. As seen in Figure 17, the total steam required for the centre injection port position was always more than that required for the bottom injection port, for the same injection rate. Also, for a fixed location of the injection port, as the injection rate increases, the total steam required decreases and converges to around 15 lbs at 100 psia and 99% steam quality. This latter value is the minimum steam required to flood the entire core with steam, under the conditions of this experiment.

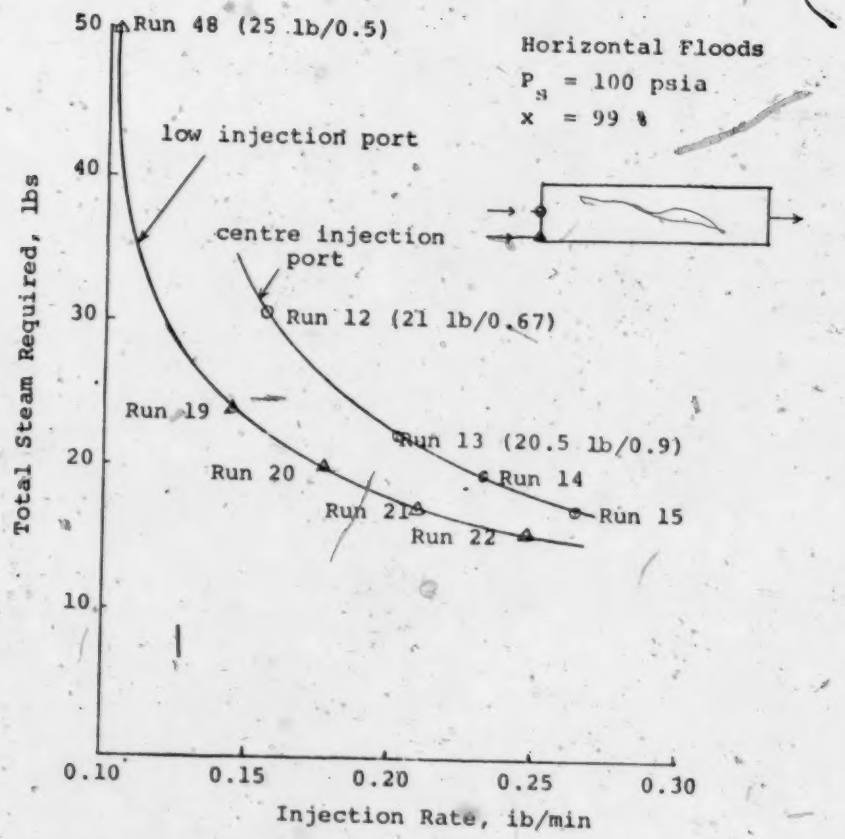

Figure 17

Effects of Injection Rate and Location of Injection Port on Total Steam Requirement to Heat the Entire Core up to the Steam Temperature

3. Effect of Dip Angle on Steam Zone Growth and Temperature Distribution

To study the behavior of steam zone growth and temperature distribution for the different dip angles, steam was injected at various dip angles from vertical downward to 40° upward at a pressure of about 100 psia, and a steam quality of about 99 %.

Figures 18A and 18B illustrate the effect of dip angle on steam zone growth. The injection rate of steam was held to approximately 0.16 lb/min. As expected, as the system becomes more horizontal, the volumetric sweep efficiency of the steam decreases. As the inclination changes further, very severe steam channelling occurs along the top of the porous medium, particularly in the cases when the angle of dip was 20° or more.

In Figures 19A and 19B it can be seen that, on the basis of the temperature distribution ater 37 minutes of steam injection, the displacement efficiency of steam is more favorable for the down dip displacement cases, and gradually decreases in efficiency as the angle changes from a downward to an upward dip. Most of the injected heat tends to remain in the steam zone in the case of down-dip floods, whereas there is a significant amount of heat stored in the water zones in the case of up-dip floods. Here again the circular cross-sections illustrated in the figures show the temperature distribution across the mid-section plane of the core normal to the direction of the injection flow.

INJECTION CONDITION :

Injection Rate: 0.133-0.168 lb/min
Inj. Steam Quality: 98% and up
Inj. Steam Press: 100-125 psia

CORE PROPERTY

Porosity : 42 %
Permeability : 19 darcies
Initial Water Sat. : 100 %

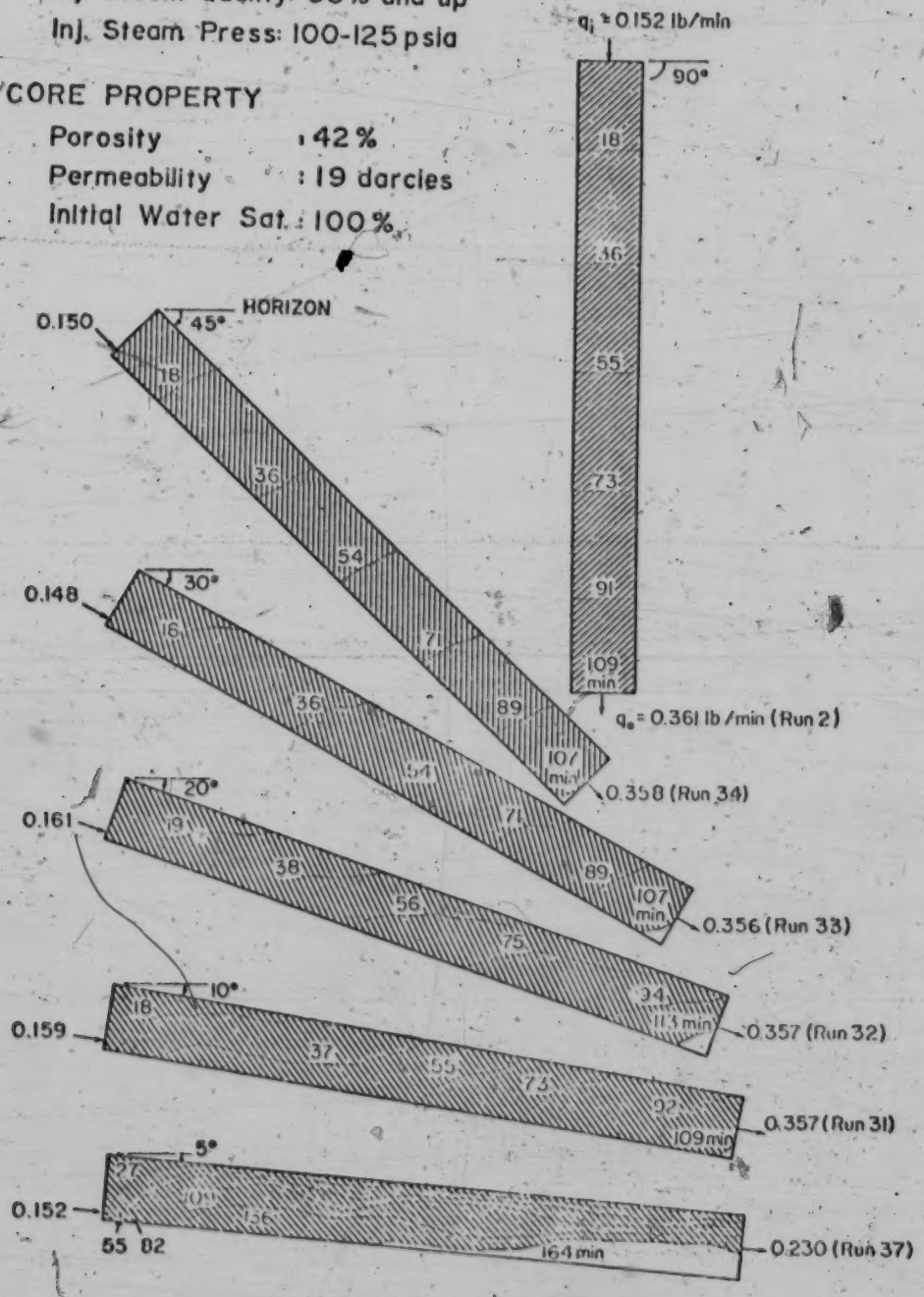

Figure 18A EFFECT OF DIP ANGLE ON STEAM ZONE GROWTH

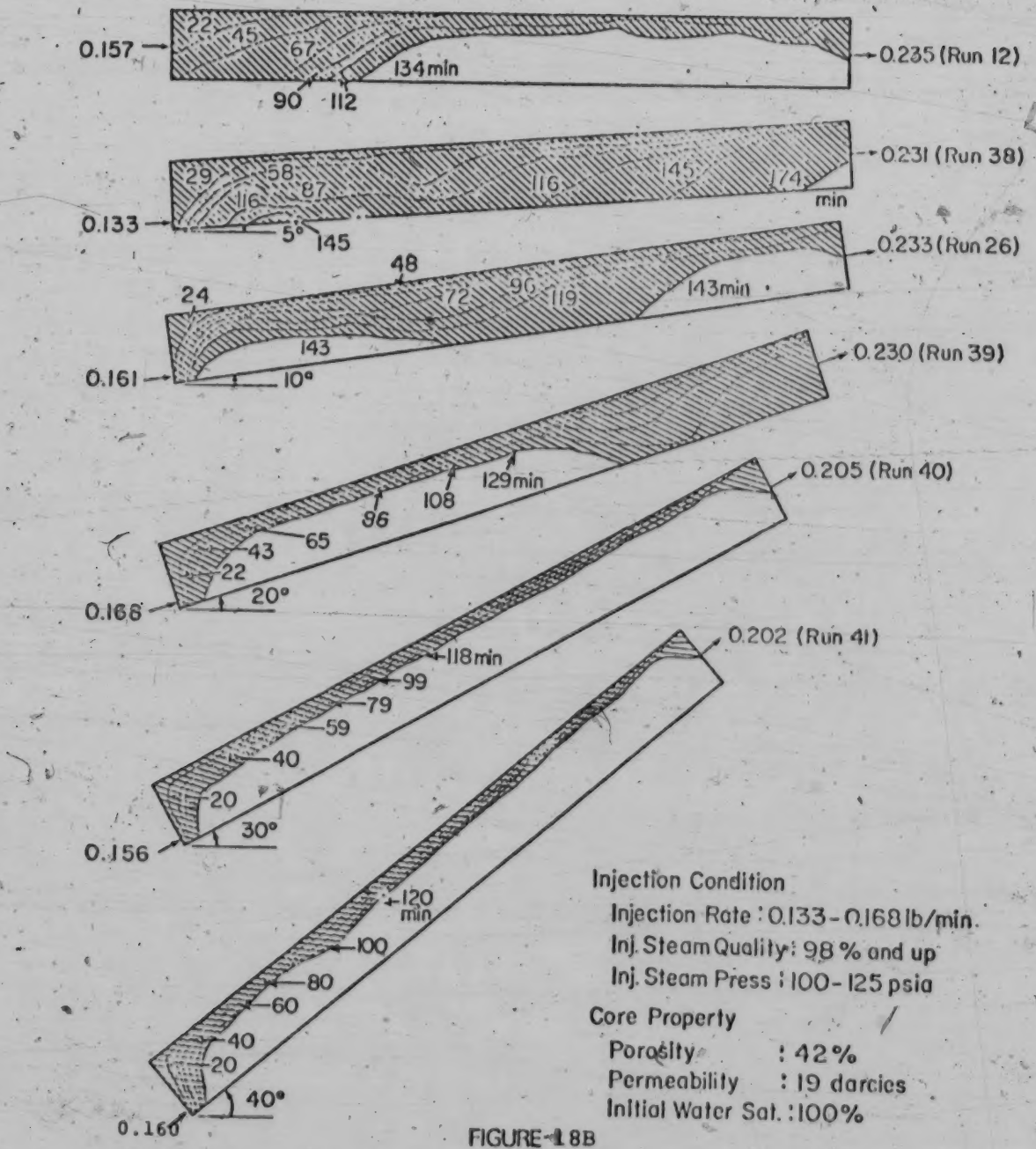

Injection Condition

Injection Rate : 0.133 - 0.168 lb/min.
Inj. Steam Quality : 98 % and up
Inj. Steam Press : 100 - 125 psia

Core Property

Porosity : 42 %
Permeability : 19 darcies
Initial Water Sat. : 100 %

FIGURE-18B

EFFECT OF DIP ANGLE ON STEAM ZONE GROWTH

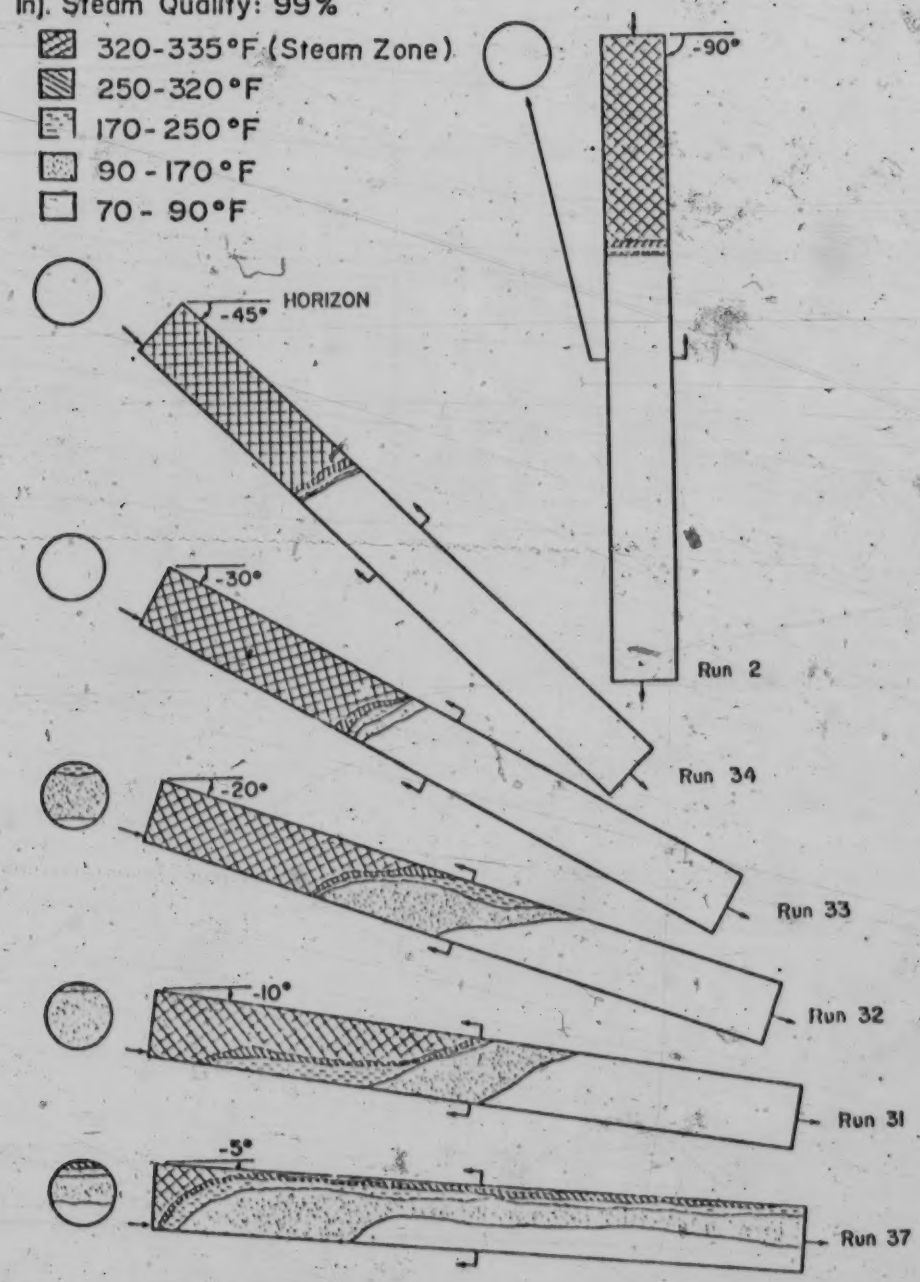

Figure 19A
TEMPERATURE DISTRIBUTION AFTER 37 MIN. OF STEAMFLOOD INTO WATER SATURATED CORE

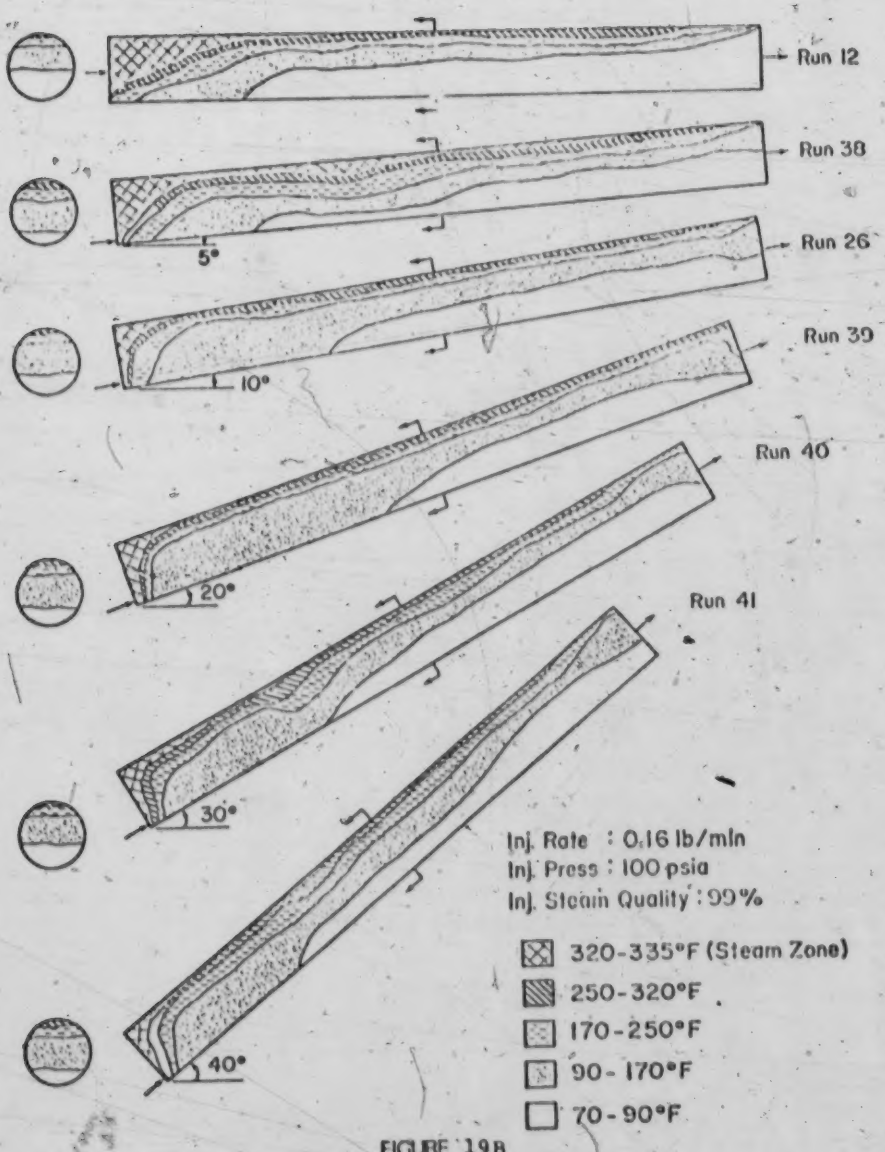

FIGURE 19B
TEMPERATURE DISTRIBUTION AFTER 37 MIN.
OF STEAMFLOOD INTO WATER SATURATED CORE

Figures 20 through 24 present another view of the temperature profiles at the injection port (#30), the centre of the middle of the core (#19), the upper end of the core (#23), and the outlet of the core (#33) for the various angles of dip. These figures present the temperature profiles relating to the 45° downward, horizontal, 10° degree upward, 30° upward, and 40° upward dip angles, respectively, injecting steam at a pressure of 100 psia, a steam quality of close to 100%, and an injection rate of approximately 0.16 lb of steam per minute.

As shown in Figure 20, the temperature profile measured at thermocouples #19, #23, and #33 as a function of time are very steep, which indicates that the water zone developed was not significant in size for this particular case. For the horizontal flood, however, as shown in Figure 21, the temperature profiles measured at thermocouples #19 and #33 tend to become less steep, indicating that the hot water zone developed was sizable. It is interesting to note that as the system becomes more inclined for the up-dip floods, the temperature profile shows a somewhat zigzag behavior, which supports the fact that the steam zone developed during the early stages of the steamflood was replaced by hot water which was developed by condensation of the steam and/or gravity segregation. This phenomenum was much more pronounced at the upper section of the porous medium (see #23 in Figures 22, 23, and 24).

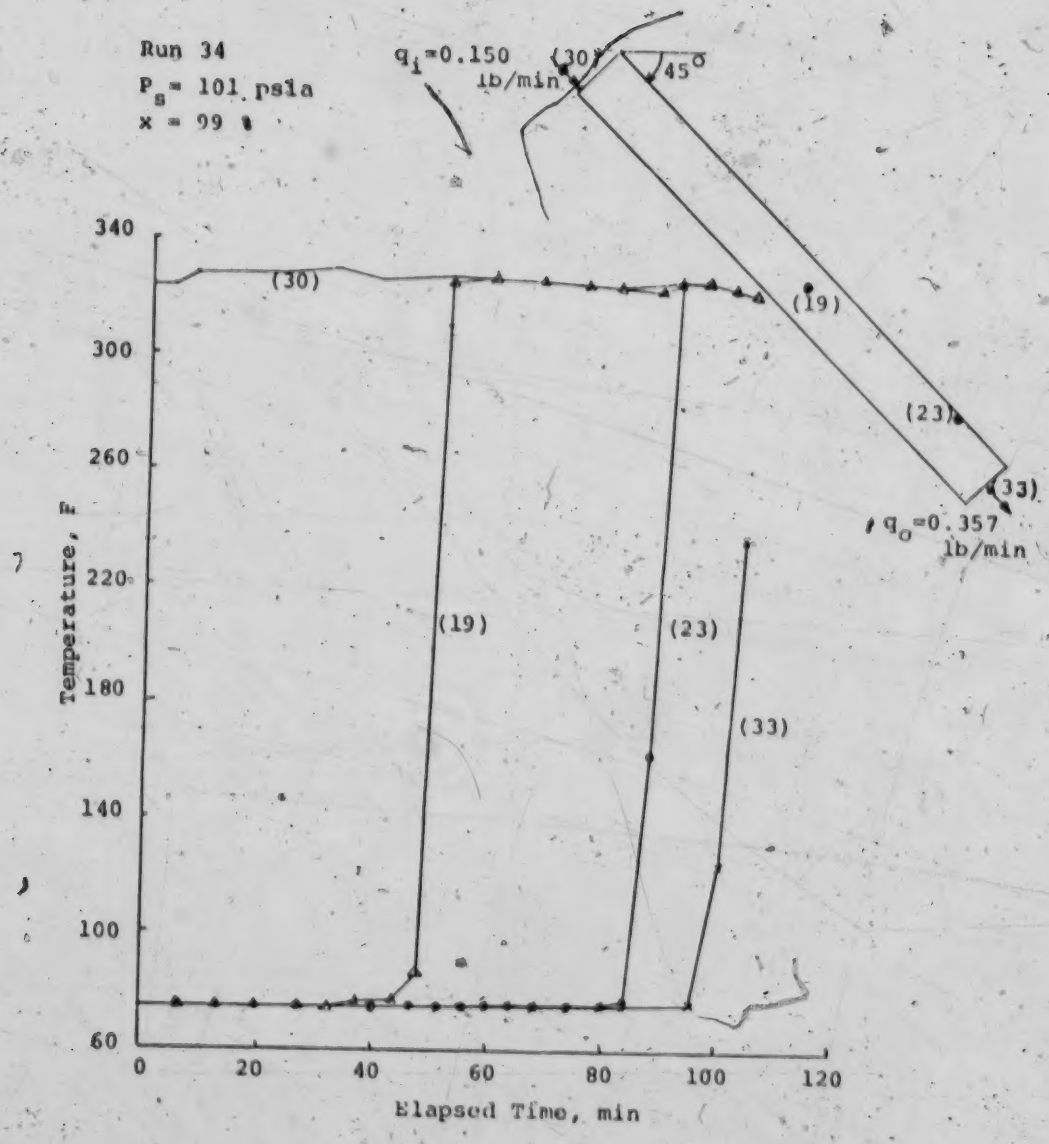

Figure 20

Temperature Profile of 45° Down Dip Flood

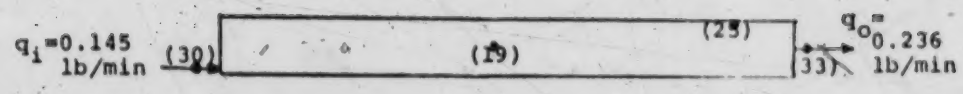

Run 19
P_s = 100 psia
x = 99 %

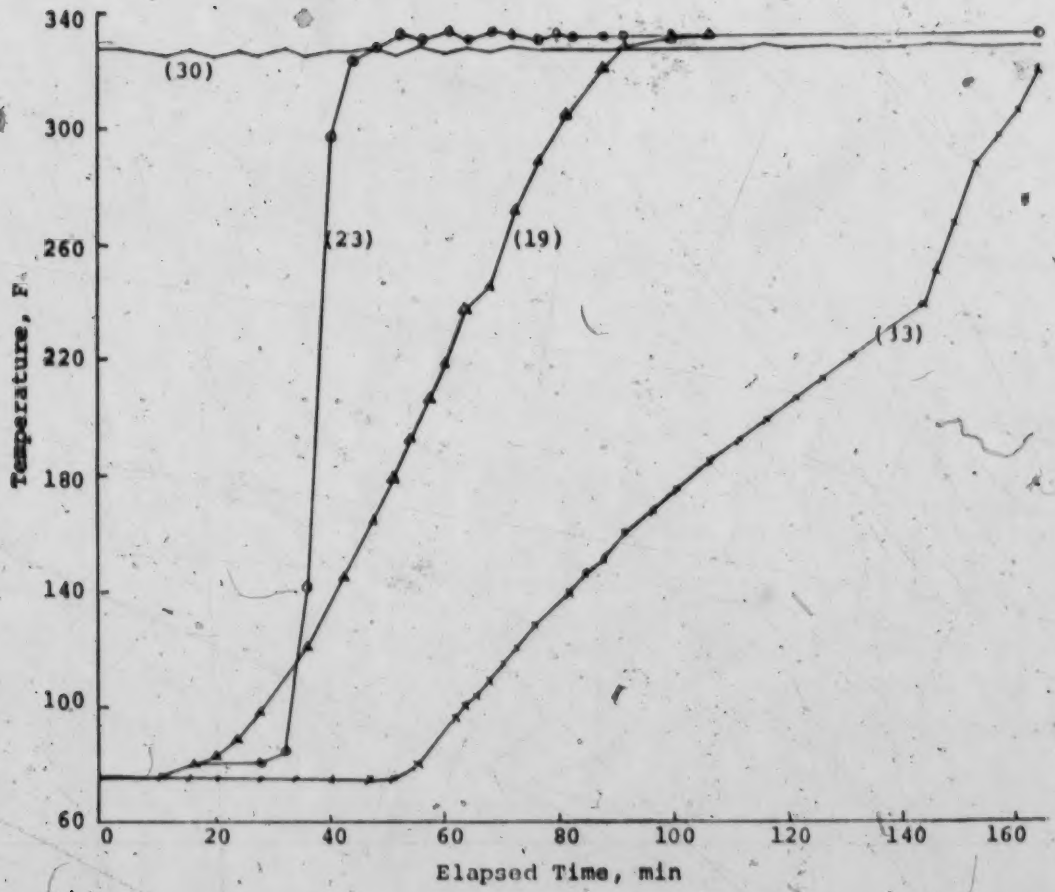

Figure 21
Temperature Profile of Horizontal Flood

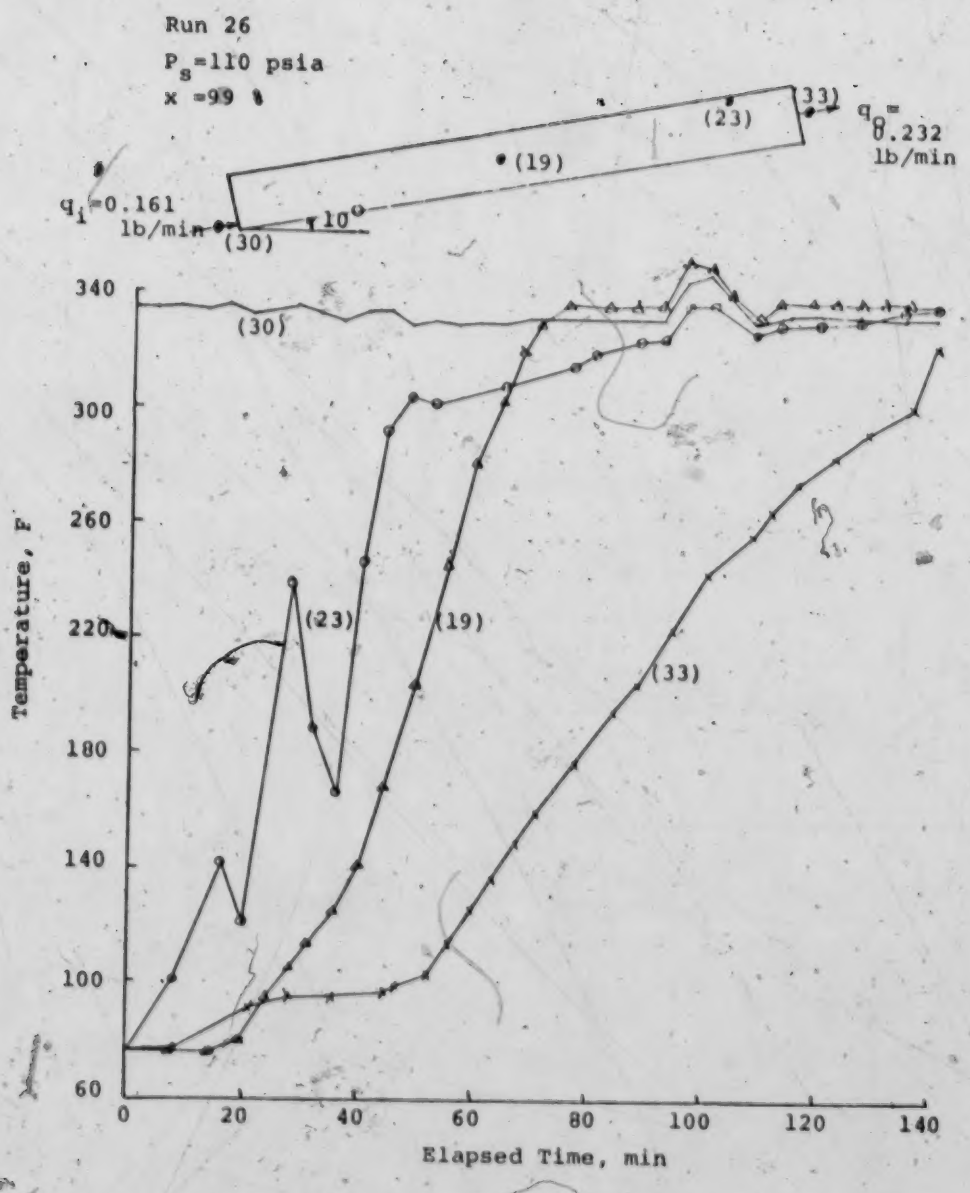

Figure 22
Temperature Profile of 10° Up Dip Flood

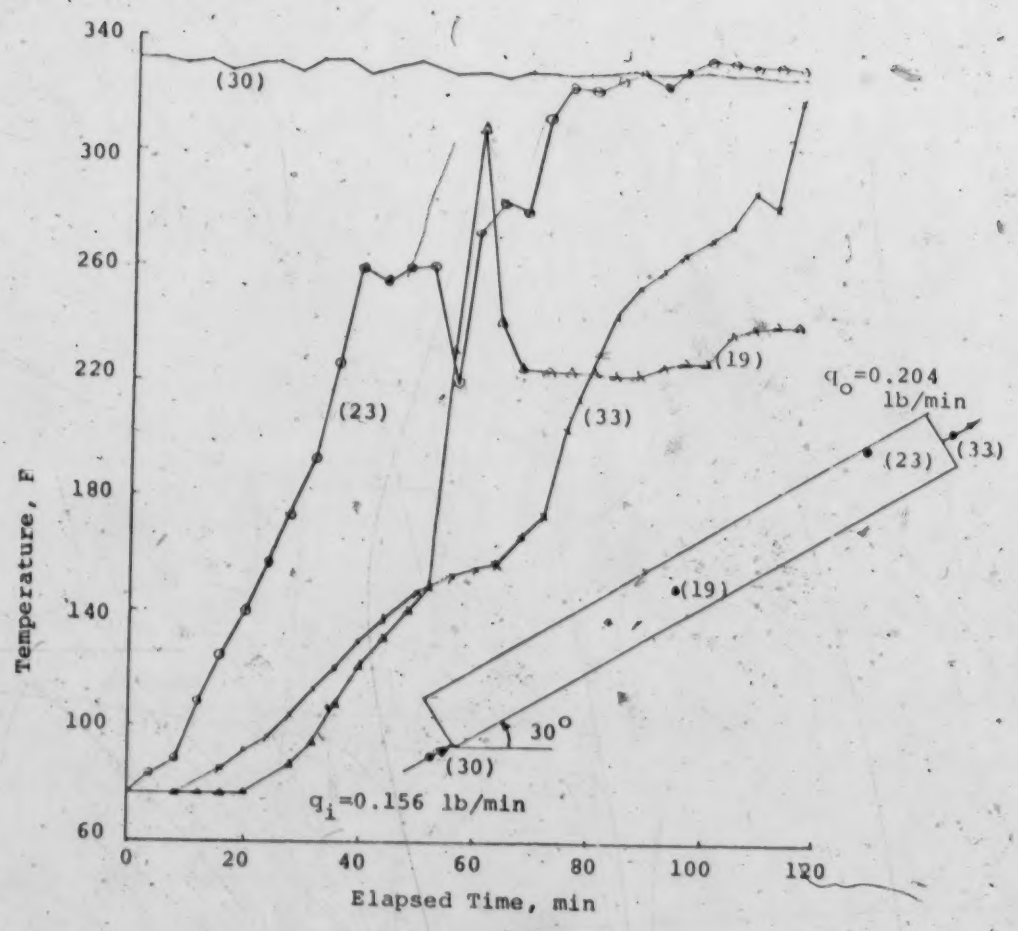

Figure 23

Temperature Profile of 30° Up Dip Flood

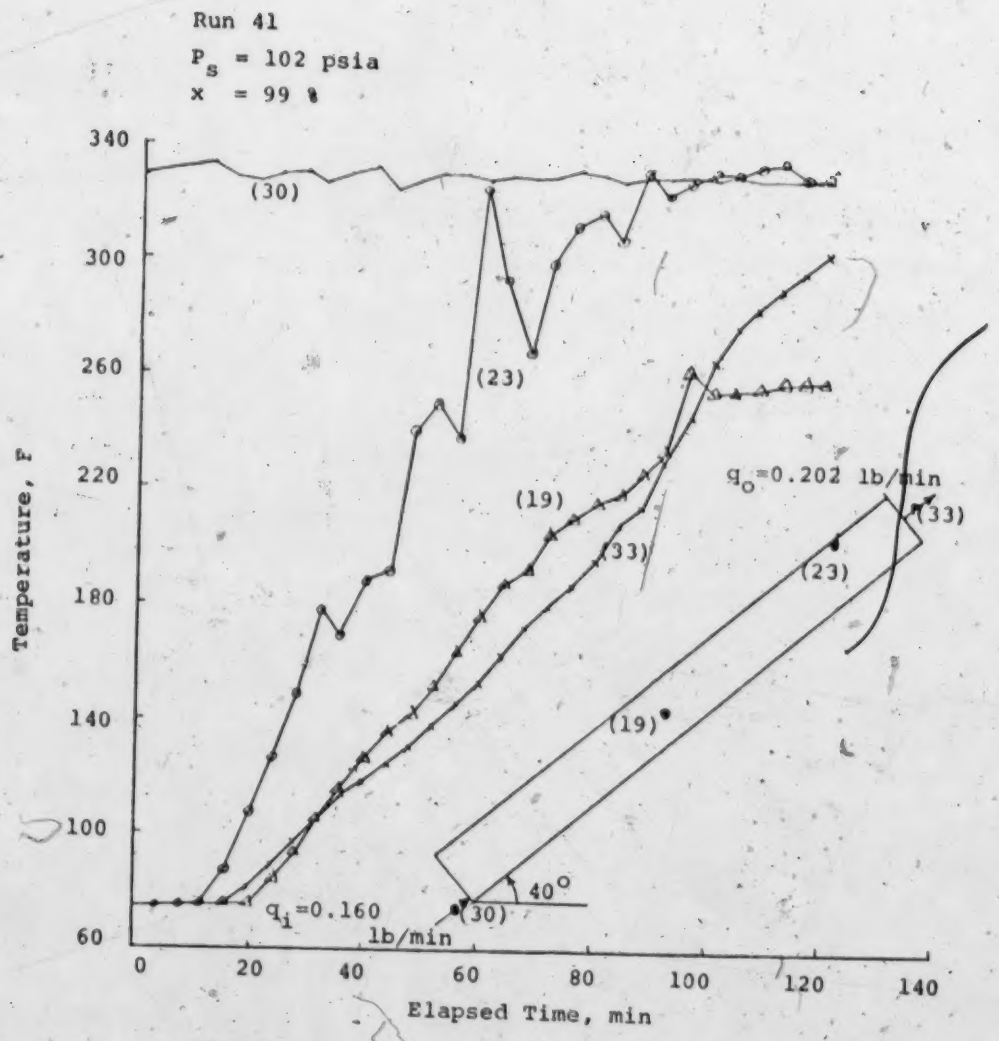

Figure 24

Temperature Profile of 40° Up Dip Flood

Effect of Injection Rate on Temperature Distribution for Inclined Porous Medium

Figure 25 demonstrates the temperature distribution after 14.4 lbs of steam was injected into a 10° up-dip-inclined porous medium at various injection rates. As illustrated in Figure 12, as the injection rate increases, the volumetric sweep efficiency by steam tends to increase. In the up-dip-inclined injection case, however, the volumetric sweep efficiency is not as much affected by the injection rate as in the case of the horizontal flood. From this result, it would be expected that for an up-dip injection, as inclination increases, the effect of the injection rate on the volumetric sweep efficiency was not as pronounced as was the case for a down-dip flood or a horizontal drive.

Even though the above experimental work has no direct field applicability, it still gives good information on the behavior of steam displacing water in a porous medium. These results could be applied to the problem of injecting steam into the water table during the early life of a tar-sands recovery project, or as a tertiary-recovery technique in a watered-out reservoir.

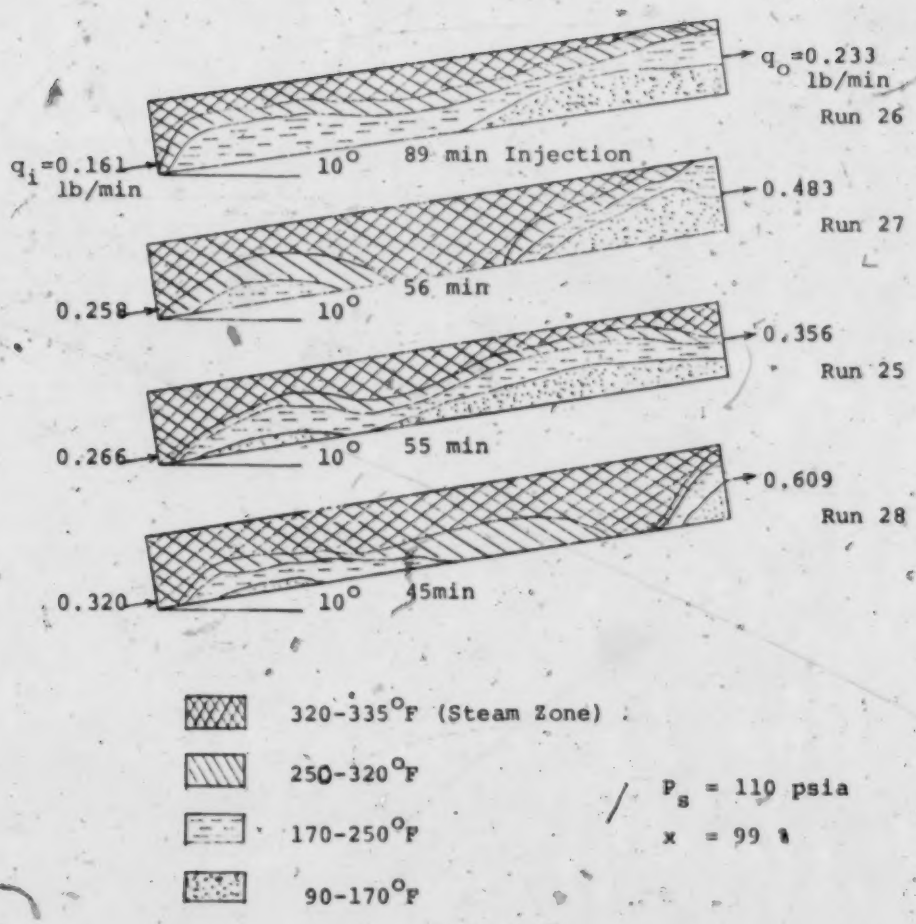

Figure 25
Temperature Distribution After 14.4 lbs of Steam was Injected into the 10° Up Dip Inclination at Various Injection Rates

CONCLUSIONS

An adiabatic linear circular model for the study of steamflooding was constructed and successfully tested.

The experiment was conducted by injecting steam into a distilled-water-saturated core to study the effect of injection rate, injection pressure, quality of steam, location of injection port, and dip angle of the porous medium on the growth of the steam zone, the temperature distribution, and the total steam required to reach steam breakthrough and to heat up the entire porous medium to steam temperature during the flooding process.

For the case of one-dimensional flow, the growth of the steam zone was principally related to the amount of the latent heat injected. The effect of the pressure and quality of the injected steam on the growth of the steam zone and/or temperature distribution was not significant over the range of steam pressures and qualities studied in this work.

For the case of two-dimensional flow, however, the growth of the steam zone and temperature distribution were sensitive to the rate of injection and the location of the injection port, but were not much affected by the pressure and quality of injected steam. That is, in the cases of the lower injection port and the higher rate of injection, the volumetric sweep efficiency was higher. Even though no direct comparison with Baker's results can be made, the rate sensitivity of the volumetric sweep efficiency agreed with

his.

The temperature distribution and the volumetric sweep efficiency during the steamflooding processes were affected significantly by the angle of dip. The displacement efficiency of steam was more favorable for the down-dip floods, and gradually decreased in efficiency as the angle changed from a downward to an upward dip. Most of the injected heat tended to remain in the steam zone in the case of down-dip floods, whereas there was a significant amount of heat stored in the water zones in the case of up-dip displacements.

The effect of the injection rate on the temperature distribution for the up-dip inclined porous medium was not as pronounced as was the case for the down-dip flood or horizontal drive.

The theoretical calculation for predicting steam quality at the down-stream of the steam line was a reliable method as long as the physical properties of the tubing and insulation were adequately known. Among the various techniques investigated for estimating steam injection rates, the method of weighing the feed tank was the simplest and the most reliable one for this particular size of apparatus.

RECOMMENDATIONS

1. The apparatus should be improved to allow direct control of the injection rate. This would avoid the inconvenience of indirectly controlling the injection rate by adjusting the production rate.

2. The study should be extended to provide for a higher pressure level of experiment by redesigning the core holder and the steam generator. Ideally, the core holder and steam generator should be designed to accomodate pressures and temperatures more representative of field conditions.

3. The experiment should be extended to include an oil-saturated core.

4. A suitable mathematical study should be carried out based on the experimental results.

5. The air or nitrogen in the feed water should be completely removed before being injected into the steam generator to ensure that there is no gas saturation within the core at any time during the experiment.

NOMENCLATURE

h	Pay thickness, ft
k_f	Thermal conductivity of overburden and substratum, Btu/hr-ft-F
l	Total length of steam line, ft
L_v	Latent heat of steam, Btu/lb
P_s	Steam pressure, psia
q_h	Heat less rate from the steam line, Btu/hr-ft
q_i	Average steam injection rate, lb/min
q_o	Average production rate, lb/min
T_i	Initial or room temperature, F
T_s	Steam temperature, F
x	Fractional steam quality at the injection port of the core
x_g	Fractional steam quality at the discharging point of the steam generator (=1.0)

REFERENCES

1. Baker, P.E., Soc. Pet. Eng. J., 89 (March, 1969).

2. Baker, P.E., Soc. Pet. Eng. J., 278 (Oct., 1973).

3. Walker, C.L., J. Can. Pet. Tech., 107 (April-June, 1965).

4. Trujano, D.N., de la Garza, B.T. and Lecona, S.C., Oil and Gas J., 83 (Jan. 21, 1974).

5. Coats, K.H., Soc. Pet. Eng., 235 (Oct. 1976).

BIBLIOGRAPHY

Adam, R.H. and Khan, A.M., "Cyclic Steam Injection Project Performance Analysis and Some Result of a Continuous Displacement Pilot", J. Pet. Tech., 95 (Jan., 1969).

Allen, J.C. and Teasdale, T.S., "Oil Recovery Process Utilizing Superheated Gaseous Mixtures", Can. Patent, No. 956885 (Oct. 29, 1974).

Allen, J.C. and Teasdale, T.S., "Oil Recovery Process Utilizing Superheated Steam", Can. Patent, No. 961409 (Jan. 21, 1975).

Baker, P.E., "Heat Wave Propagation and Losses in Thermal Oil Recovery Processes", 7th World Petroleum Congress, 3, 459. Mexico (1967).

Baker, P.E., "An Experimental Study of Heat Flow in Steam Flooding", Soc. Pet. Eng. J., 89 (March, 1969).

Baker, P.E., "Effect of Pressure and Rate on Steam Zone Development in Steamflooding", Soc. Pet. Eng. J., 274 (Oct., 1973).

Blevins, T.R., Aseltine, R.J. and Kirk, R.S., "Analysis of a Steam Drive Project, Inglewood Field, California", J. Pet. Tech., 1141 (Sept., 1969).

Blevins, T.R. and Billingsley, R.H., "The 10 Patterns Steam Flood", SPE 4756, Presented at the 45th Annual California Regional Meeting, Ventura, California (April 2-4, 1975).

Burns, W.C., "Water Treatment for Once-Through Steam Generators", J. Pet. Tech., 417 (April, 1965).

Bursell, C.G., "Steam Displacement - Kern River Field", J. Pet. Tech., 1225 (Oct., 1970).

Bursell, C.G. and Pittman, G.M., "Performance of Steam Displacement at Kern River Field", SPE 5017, 49th Annual SPE of AIME Fall Mtg., Houston, (Oct. 6-9, 1974).

Bursell, C.G., Taggert, H.J. and DeMirjian, H.A., "Thermal Displacement Tests and Results, Kern River Field, California", Producers Monthly, 18 (Sept., 1966).

Chappelear, J.E. and Volek, C.W., "The Injection of a Hot Liquid Into a Porous Medium", Soc. Pet. Eng. J., 100 (March, 1969).

Coats, K.H., "Simulation of Steamflooding with Distaillation and Solution Gas", J. Pet. Tech., 235 (Oct. 1976).

Coats, K.H., George, W.D., Chu, Chieh and Marcum, B.E., "Three-Dimensional Simulation of Steamflooding", Soc. Pet. Eng. J., 573 (Dec., 1974).

de Haan, H.J. and Schenk, L., "Performance Analysis of a Major Steam Drive Project in the Tia Juana Field, Western Venezuela", J. Pet. Tech., 111 (Jan., 1969).

Dillabough, J.A. and Prats, M., "Recovering Bitumen from Peace River Depposits", Oil & Gas J., Nov. 11, 186(1974).

Edmondson, J.A., "Effect of Temperature on Waterflooding", J. Can. Pet. Tech., 236 (Oct.-Dec., 1965).

Emergy, M.N., "Small Steam Flood Works for Independent", Pet. Eng., 63 (Sept., 1966).

Fanaritis, J.P. and Kimmel, J.D., "Review of Once-Through Steam Generators", J. Pet. Tech., 409 (April, 1965).

Farouq Ali, S.M., Secondary and Tertiary Oil Recovery Processes, Chapter VI. Steam Injection, Interstate Oil Compact Commission, Oklahoma City, Okla. (Sept. 1974). p.174.

Fitzgerald, B.M., "Surface Injection and Producting Systems for Steam Generators", Producers Monthly, 18 (Dec., 1967).

French, M.S. and Howard, R.L., "The Steamflood Job Hefner, in Sho-Vel-Tum", Oil & Gas J., 64 (July 17, 1967).

Hagoort, J., Leijnse, A. and Van Poelgeest, F., "Steam-Strip Drive: A Potential Tertiary Recovery Process", J. Pet. Tech., 1409 (Dec., 1976).

Hall, A.L. and Bowman, R.W., "Operation and Performance of Slocum Field Thermal Recovery Project", J. Pet. Tech., 402 (April, 1973).

Hearn, C.L. "The El-Dorado Steam Drive -- a Pilot Tertiary Recovery Test", J. Pet. Tech. 1377 (Nov., 1972).

Long, R.J., "Case History of Steam Soacking in the Kern River Field, California", J. Pet. Tech., 989 (Sept, 1965).

Marx, J.W. and Langenheim, R.H., "Reservoir Heating by Hot Fluid Injection", Trans. AIME, 216, 312 (1959).

Ozen, A.S. and Farouq Ali, S.M. "An Investigation of the Recovery of the Bradford Crude by Steam Injection", J. Pet. Tech., 692 (June, 1969).

Pollock, C.B. and Buxton, T.S., "Performance of a Forward Steam Drive Project - Nugget Reservoir, Winkleman Dome Field, Wyoming", J. Pet. Tech., 35 (Jan., 1969).

Pollock, C.B. and Buxton, T.S., "Winkleman Dome Steam Drive a Success", Oil & Gas J., 151 (Aug. 10, 1970).

Rincon, A.C., Diaz-Nuoz, J. and Farouq Ali, S.M. "Sweep Efficiency in Steamflooding", J. Can. Pet. Tech., 175 (July-Sept., 1970).

Satter, A. and Parrish, D.R., "A Two-Dimensional Analysis of Reservoir Heating by Steam Injection", Soc. Pet. Eng. J., 11 (2), 185 (June, 1971).

Shutler, N.D., "Numerical Three-Phase Simulation of Linear Steamflooding Process", Soc. Pet. Eng. J., 232 (June, 1969).

Shutler, N.D., "Numerical Three-Phase Model of the Two-Dimensional Steamflood Process", Soc. Pet. Eng. J., 405 (Dec., 1970).

Shutler, N.D. and Boberg, T.C., "A One-Dimensional Analytical Technique for Predicting Oil Recovery by Steamflooding", Soc. Pet. Eng. J., 489 (Dec., 1972).

Smith, R.V., Bertuzzi, A.F., Templeton, E.F. and Clampitt, R.L., "Recovery of Oil by Steam Injection in the Smackover Field, Arkansas", J. Pet. Tech., 883 (Aug., 1973).

Trujano, D.N., de la Garza, B.T. and Lecona, S.C., "How Ambient Conditions Affect Steam-Line Heat Loss", Oil & Gas J., 83 (Jan. 21, 1974).

Valleroy, V.V., Willman, B.T., Campbell, J.B. and Powers, L.W., "Deerfield Pilot Test of Oil Recovery by Steam Drive", J. Pet. Tech., 956 (July, 1967).

van Dijk, C., "Steam-Drive Project in the Schoonebeek Field, the Netherlands" J. Pet. Tech., 295 (March, 1968).

Volek, C.W. and Pryor, J.A., "Steam Distillation Drive - Brea Field, California", J. Pet. Tech. 899 (Aug., 1972).

Walker, C.L., "The Chemical Treatment of Water used in Steam Injection Systems", J. Can. Pet. Tech., 107 (April-June, 1965).

Willman, B.T., Valleroy, V.V., Runberg, G.W., Cornelius, A.J. and Powers, L.W., "Laboratory Studies of Oil Recovery by Steam Injection", Trans., AIME, 222, 681 (1961).

APPENDICES

APPENDIX A

Steam Quality Calculation at Injection Port

Steam quality at the injection port may be calculated from Equation (A-1):

$$x = x_g - q_h l / L_v q_i \qquad (A-1)$$

where, x = the steam quality at the injection port of the core

x_g = the steam quality at the discharge point of the steam generator (=1.0)

q_h = the heat loss rate from the steam line, Btu/hr-ft

l = total length of the steam line, ft.

q_i = the average mass flow rate of the steam, lb/hr

L_v = the latent heat of the steam at the average line pressure, Btu/lb.

If l, L_v, and q_i are known, q_h must be known to calculate x.

The heat loss from the steam line consists of the heat transfer by radiation and heat loss due to the convection to the surroundings.

Heat Loss by Radiation

The heat transport by radiation can be written as:

$$q_r = 0.1713 \times 10^{-8} \left[(T_{surf} + 460)^4 - (T_a + 460)^4 \right] \qquad (A-2)$$

where, q_r = the heat loss rate by radiation, Btu/hr-ft

0.1713×10^{-8} = the Boltzman's constant, Btu/hr-ft²-R⁴

A = the exterior surface area, ft²/ft

e = the emissivity (=1 for the black body)

T_{surf} = the exterior surface temperature, F

T_a = the ambient temperature, F.

Rearranging Equation (A-2), one can obtain:

$$q_r = 0.1713 \times 10^{-8} \, Ae \left[(T_{surf} + 460)^2 + (T_a + 460)^2\right] \times \left[(T_{surf} + 460) + (T_a + 460)\right](T_{surf} - T_a)$$

or $$q_r = Ah_r(T_{surf} - T_a) \qquad (A-3)$$

where, $$h_r = 0.1713 \times 10^{-8} e \left[(T_{surf}+460)^2 + (T_a+460)^2\right] \times \left[(T_{surf}+460) + (T_a+460)\right] \qquad (A-4)$$

(= the heat transfer coefficient by radiation, Btu/hr-ft²-R).

Heat Loss by Convection

The convectional heat transfer may be expressed as:

$$q_c = Ah_c(T_{surf} - T_a) \qquad (A-5)$$

where, q_c = the heat loss rate by convection, Btu/hr-ft

h_c = the heat transfer coefficient by convection, Btu/hr-ft²-R and is given by the Nusselt number*

$$\frac{h_c d}{K_a} = 0.53 \left[d^3 (T_{surf} - T_a) \frac{gB_a}{V_a^2} \cdot Pr\right]^{1/4}$$

* McAdams, W. H., Heat Transmission, McGraw-Hill Book Co., New York (1954), Third Edition. pp. 172-176.

(A-6)

where, d = outside diameter of steam line surface, ft

K_a = thermal conductivity of air at T_{avg}, Btu/hr-ft-R

g = acceleration due to gravity (=4.17x10^8 ft/hr^2)

B_a = coefficient of volumetric expansion of air at T_{avg}, R^{-1}

V_a = kinematic viscosity of air of T_{avg} (μ_a/ρ_a), ft^2/hr

μ_a = dynamic viscosity of air at T_{avg}, lb/ft-hr, (=2.42xc.p.)

ρ_a = density of the air at T_{avg}, lb/ft^3

Pr= Prandtl number ($=\frac{C_{pa}\mu_a}{K_a}$)

C_{pa} = specific heat capacity of air at constant pressure and T_{avg}, Btu/lb-R

$T_{avg} = (T_{surf} + T_a)/2.$

At 14.7 psia,

$K_a = 0.01328 + 2.471\times10^{-5}T - 4.247\times10^{-9}T^2$

$\rho_a = 0.0771 - 8.848\times10^{-5}T - 3.744\times10^{-8}T^2$

$\mu_a = 0.0400 + 6.155\times10^{-5}T - 1.220\times10^{-8}T^2$

$C_{pa} = 0.2382 + 1.390\times10^{-5}T + 1.027\times10^{-8}T^2$

$B_a = 0.0024 - 0.75\times10^{-5}T + 0.169\times10^{-7}T^2 - 0.148\times10^{-10}T^3$

$g = 4.17\times10^8$

$T = T_{avg}$.

Heat Loss Rate

Thus the total heat loss to the surroundings,

$q = q_c + q_t$

= heat conduction rate through the tube

wall and the insulation,

or, $q = AU(T_s - T_a)$ (A-7)

where, q = total heat loss rate, Btu/hr-ft

U = overall heat transfer coefficient, Btu/hr-ft²-R

$$= \left[\frac{d}{d_i h_i} + \frac{d}{2}\frac{\ln(d_o/d_i)}{K_{tube}} + \frac{d}{2}\frac{\ln(d/d_o)}{K_{ins}} + 1/(h_c+h_r)\right]^{-1} \quad \text{(A-8)}$$

where, d_o = outside tube diameter, ft

d_i = inside tube diamter, ft

K_{tube} = thermal conductivity of steam line tube, Btu/hr-ft-R

h_i = inside film heat transfer coefficient (3000-5000 Btu/hr-ft²-R)

K_{ins} = thermal conductivity of insulation, Btu/hr-ft-R

d = total diameter after insulation, ft

T_s = steam temperature, R

T_a = ambient temperature, R.

Since h_i and K_{tube} are large numbers, one might approximate U as:

$$U = \left[\frac{d}{2}\frac{\ln(d/d_o)}{K_{ins}} + \frac{1}{h_c + h_r}\right]^{-1} \quad \text{(A-9)}$$

Moreover for the bare tube:

$$U = \left[\frac{1}{h_c + h_r}\right]^{-1} \quad \text{(A-10)}$$

Since, $q = AU^*(T_s - T_{surf})$ (A-11)

where, $$U^* = \left[\frac{d}{d_i h_i} + \frac{d}{2}\frac{\ln(d_o/d_i)}{K_{tube}} + \frac{d}{2}\frac{\ln(d/d_o)}{K_{ins}}\right]^{-1}$$

(A-12)

= overall heat transfer coefficient from the inside of tube to the exterior surface of the insulation, Btu/hr-ft²-R.

Therefore,

$$T_{surf} = T_s - \frac{q}{AU^*} \quad (A-13)$$

The value of T_{surf} calculated from Equation (A-13) is compared with the measured value, and if the two do not agree within a few degrees, the physical properties, like K_{tube}, A, and/or T_{surf}, are adjusted until the result is satisfied. The final values of the properies are used to calculate the heat loss rate q. Now Equation (A-1) is furnished for the calculation of steam quality at the injection port of the core.

To test the accuracy of this calculation method, an adiabatic calorimeter was constructed for the comparison of the steam quality measured with the calculated steam quality.

The calorimeter consisted of four thermocouples to measure the temperatures at the upstream and downstream end of the steam line and cooling water line, a calibrated high pressure gauge, a twenty-foot-long stainless steel cooling coil, a cooling water jacket, and four inches of insulation (styrofoam chips) surrounding the outside of the jacket. After steady state had been reached, temperatures at the inlet and outlet ends of the steam and cooling water lines, pressure at the inlet of the steam line and flow rates of

the cooling water and steam were measured.

The measured data were used in the following equations to calculate steam quality at the inlet of the calorimeter or at the end of the steam line:

(rate of heat gain of the cooling water)

(rate of heat loss to surroundings)

= (rate of heat loss of the steam) (A-14)

$$\dot{H}_w = q_w C_w (T_{w2} - T_{w1}) \quad \text{(A-15)}$$

$$\dot{H}_s = q_s \left[H_{w,Ts1} + xL_v - C_{sc}(T_{s2} - 32) \right] \quad \text{(A-16)}$$

where,

$\dot{H}_w$ = rate of enthalpy gain of the cooling water, Btu/lb-min

$\dot{H}_s$ = rate of enthalpy loss of the steam, Btu/lb-min

q_w = flow rate of cooling water, lb/min

q_s = flow rate of steam, lb/min

T_{w2} = outlet temperature of cooling water, F

T_{w1} = inlet temperature of cooling water, F

C_w = average heat capacity of cooling water between inlet and outlet temperatures, Btu/lb-F

$H_{w,Ts1}$ = enthalpy of saturated water at steam temperature, Btu/lb

x = steam quality at the inlet of the calorimeter, fractional

L_v = latent heat of steam at the inlet condition, Btu/lb

C_{sc} = average heat capacity of steam condensate between outlet temperature of the steam condensate and 32 F, Btu/lb-F

T_{s2} = outlet temperature of steam condensate, F.

Inserting Equations (A-15) and (A-16) into Equation (A-14) and setting the rate of heat loss to surroundings equal to zero - since it is an adiabatic calorimeter - and solving for x, one can obtain:

$$x = \frac{1}{L_v}\left[\frac{q_w}{q_s} C_w(T_{w2} - T_{w1}) - H_{w,Tsl} + C_{sc}(T_{s2} - 32)\right] \qquad (A-17)$$

To compare the results obtained from the calculated steam quality (Equation A-1), with the results obtained from the experimental test (Equation A-17), a 20-foot-long stainless steel tube was employed. The tube had an 0.18-inch inside diameter and a 0.25-inch outside diameter. The first 9 feet of the tube was insulated with fibre glass tube insulator and the remaining length with asbestos tape. This resulted in an outside diameter of 2.5 inches over the entire steamline. In addition, the entire steamline was sheathed with aluminum foil to reduce radiation heat loss.

The physical properties used in calculation were:

K_{tube} = 26 Btu/F-hr

$K_{fibre\ glass}$ = 0.032 Btu/F-hr

$K_{asbestos}$ = 0.110 Btu/F-hr

ε = 0.3 (emissivity of aluminum)

h_i = 3500 Btu/F-hr-ft^2.

Table A presents the experimentally determined steam quality and the calculated steam quality. The results were plotted in Figure A for comparison. As shown in Figure A,

the calculated steam quality agreed very well with the experimental results, indicating that the calculation method to determine steam quality at the injection port was reliable.

TABLE A

Comparison of Steam Quality: Measured vs. Calculated

T_{w1}, F	T_{w2}, F	T_{s1}, F	T_{s2}, F	P_s, psia	q_w, lb/min	q_s, lb/min	x^*_{exp}	x^{**}_{cal}
61	100	295	70	65.5	3.25	0.124	0.884	0.883
60	116	288	72	58.9	3.25	0.173	0.913	0.917
60	145	264	75	40	3.24	0.256	0.934	0.937
60	85.5	297	69	67.5	3.23	0.085	0.825	0.828
60	67	298	70	68.6	3.24	0.032	0.527	0.548
57	96	332	67	111	3.23	0.123	0.862	0.867
57	130	328	69	105	3.24	0.224	0.915	0.933
57	77	38	70	224	3.23	0.072	0.707	0.694
58	122.5	390	69	227	3.23	0.197	0.898	0.896
59	75	420	71	315	3.23	0.062	0.599	0.589
58	151	420	76	315	3.21	0.275	0.925	0.914
74	169	242	102	27	3.22	0.285	0.943	0.932
64	161	240	90	26	3.20	0.286	0.946	0.931
63	158	242	88	27	3.27	0.286	0.948	0.937
63	154	256	80	35	3.15	0.264	0.945	0.936
61	135	278	75	50	3.19	0.218	0.941	0.932
59	107	295	67.5	66	3.22	0.148	0.904	0.902
60	93	300	67	71	3.09	0.101	0.859	0.856
59	69.5	300	70	71	3.32	0.042	0.657	0.655
59.5	67	335	70	115	3.33	0.035	0.511	0.507
59	90	339	66	122	3.31	0.103	0.837	0.836
59	112	335	67	115	3.37	0.171	0.899	0.907
59	129	322	73	111	3.31	0.216	0.932	0.930
59	150	328	72	105	3.35	0.281	0.946	0.947
59	182	312	85	84	3.37	0.381	0.962	0.965
62	75	367	71	173	3.33	0.052	0.634	0.616
60	95	366	68	171	3.37	0.117	0.846	0.838
60	105	367	67	173	3.37	0.147	0.876	0.873
60	122	367	70	173	3.43	0.203	0.893	0.912
60	137	365	72	169	3.35	0.400	0.929	0.929
60	175	358	71	155	3.45	0.358	0.968	0.959

* from Equation (A-17) - experimentally measured

** from Equation (A-1) - theoretically calculated

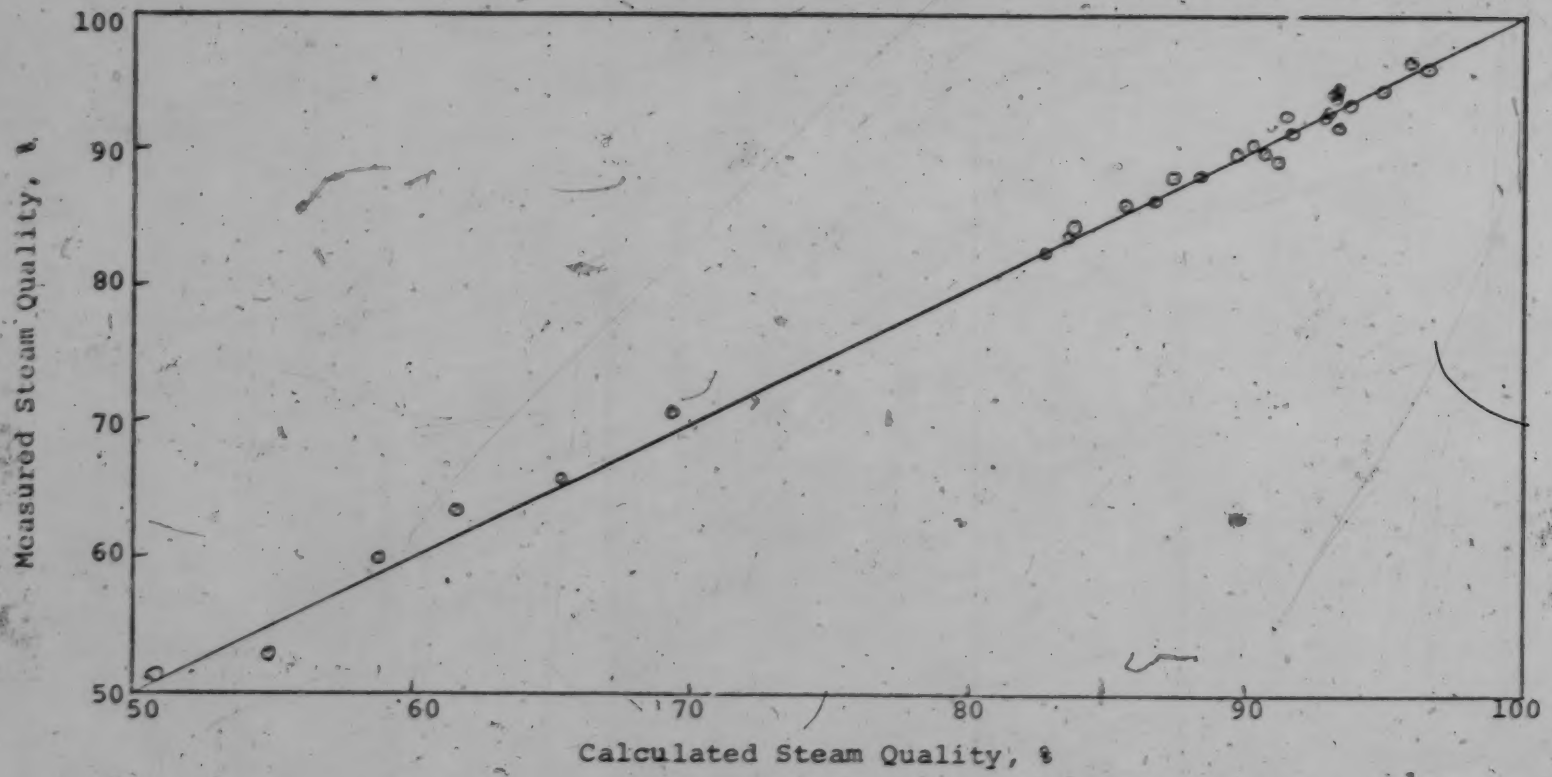

Figure A

Comparison of Steam Quality Determinations

APPENDIX B

Comparison of Various Calculation Techniques for Injection Rate of Steam

Four different methods were independently employed to measure the injection rate of steam.

1. Standard Method (Material Balance Method)

Making a material balance over the core as shown in following equation, the total injected steam for a run can be calculated:

(weight of total steam injected)
+
(weight of initial water in the core)
= (weight of total water produced)
+
(weight of amount of water left in the core after the run)

(B-1)

The initial amount of water in the core is equivalent to the pore volume of the core. The final amount of water left in the core after a run can be determined from the difference between the initial amount of water in the core and the amount of water required to refill the core to 100 % saturation. This refilling can be easily achieved by allowing the core to cool for a certain time period, which generates a partial vacuum due to the condensation of steam, and then allowing water to imbibe into the core.

Solving the above Equation (B-1) for the weight of the total steam injected and dividing it by the total

time for the run, one obtains the average injection rate of steam.

2. Weighing Method

The total amount of water supplied to the steam generator from the feed tank during the injection period may be measured by ascertaining the reduction in the weight of the water in the feed tank. The total reduction of the weight of the feed tank is divided by the given time interval to give an average production rate of steam during the given time interval.

3. Power Rating Method

The electrical energy input through the three phase electrodes can be calculated from the following equation:

$$W = \sqrt{3}EIt \quad \text{joules or watts-sec} \qquad (B-2)$$

where, E = volts (=206 volts on average)

I = amperes (read from an ammeter)

t = seconds (cumulative heating time)

or $W = (1\ \text{Btu}/1055\ \text{joules})(1.732)(206)(60)\ It$
$= 20.29\ It\ \ \text{Btu}$ (B-3)

where, t = minutes.

The net electrical heat utilized may be calculated from following equation:

(net electrical heat utilized) = (electric heat input)
- (heat loss of steam generator to surroundings)

(B-4)

To evaluate the heat loss of the steam generator to the surroundings, the steam generator was set for various pressures, without introducing feed water into it and with no production of steam from it. Measuring the average current and the cumulative heating time, the total heat loss was calculated from Equation (B-3). The total heat loss may be divided by the total time elapsed for the test to give the average heat loss rate.

Table B-I shows the experimental calibration data for heat loss from the steam generator, and the results are presented in Figure B-1.

At the steady state of the steam generator, the sum of the net electrical heat utilized and the enthalpy introduced by the injection of feed water is the same as the enthalpy out due to the production of 100 % steam at the given condition of the steam generator, i.e.,

(net electrical heat utilized) = (heat out due to the production of 100 % steam at given generator condition)

- (enthalpy introduced by the water injected into the steam generator)

(B-5)

The enthalpy introduced by the feed water into the steam generator can be obtained from the following Equation (B-6):

TABLE B-I

Calibration Data for Heat Loss of Steam Generator

$$W = 20.29 \cdot I \cdot t \quad \text{Btu}$$

$$W_{loss} = W/T \quad \text{Btu/min}$$

Run	P, psig	I, amp	t*, min	T**, min	W_{loss}, Btu/min
1	56	50	20.40	300.24	68.93
2	185	106	13.18	270.30	104.87
3	86	61.5	41.24	661.49	77.80
4	92	70	38.30	686.70	79.22
5	92	73	42.24	794.53	78.74
6	145	92	48.90	1,001.42	91.15
7	124	85	48.74	966.54	86.97
8	165	103	57.11	1,192.30	100.10
9	90	73	49.15	940.61	77.40
10	90	73.5	44.84	864.34	77.37
11	72	69	54.76	1,025.40	74.77
12	50	56	58.25	1,034.21	64.00
13	151	74	71.10	1,109.53	96.22
14	200	94	23.21	394.80	112.13

* cumulative heating time

** total elapsed time for the test

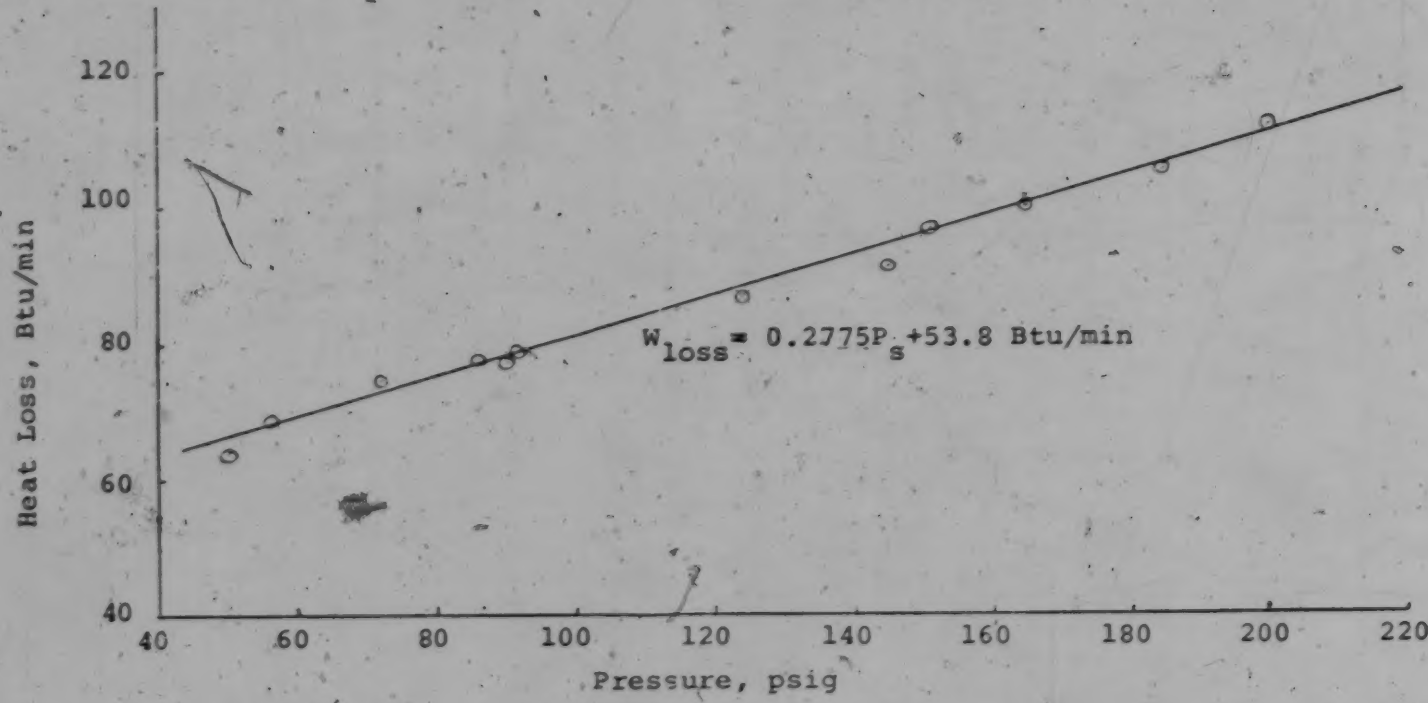

Figure B-1

Heat Loss of Steam Generator to Surroundings

$$H_w = C_w (T-32) \text{ (weight of feed water)} \qquad \text{(B-6)}$$

where,

H_w = enthalpy of entering water, Btu

C_w = average heat capacity of water between T and 32 F, Btu/lb-F

T = temperature of injected water,

weight of feed water = obtained from ascertaining the reduction of the weight of the feed tank.

Combining Equations (B-4) and (B-5) and solving for heat out due to the production of 100 % steam at the given condition of the steam generator, the amount of steam generated can be calculated. The average injection rate of steam then can be obtained from the following equation:

$$q_i = H_p / h_s / t \qquad \text{(B-7)}$$

where,

q_i = average injection rate of steam (= average production rate of steam), lb/min

H_p = total heat out due to the 100% steam generation, Btu

h_s = specific enthalpy of 100 % steam, Btu/lb

t = total elapsed time of interest, min.

4. Pitot Tube Flow Meter Method*

---

* Notations in this section may be obtained from any thermodynamic textbook.

The force-momentum balance equation can be expressed as:

$$v\,dp + dz + u\,du/g_c + dP + dW_s = 0 \,, \qquad (B\text{-}8)$$

while the first law of thermodynamics can be written as:

$$\Delta H + \Delta z + \Delta u^2/2g_c = Q - W_s \,. \qquad (B\text{-}9)$$

If there is no shaft work and no friction loss, and if the potential energy term is negligible, Equation (B-8) becomes:

$$-v\,dp = u\,du/g_c \qquad (B\text{-}10)$$

Further, if the system is adiabatic, Equation (B-9) becomes:

$$-dH = u\,du/g_c \,. \qquad (B\text{-}11)$$

Integrating Equations (B-10) and (B-11), one can obtain:

$$-\int_{P_1}^{P_2} v\,dp = (u_2^2 - u_1^2)/2g_c \qquad (B\text{-}12)$$

and

$$-\Delta H = (u_2^2 - u_1^2)/2g_c \,. \qquad (B\text{-}13)$$

However,

$$-\Delta H = -\int_{T_1}^{T_2} C_p\,dT \qquad (B\text{-}14)$$

and furthermore for an ideal gas,

$$-\int_{T_1}^{T_2} C_p\,dT = \frac{k}{k-1} R(T_1 - T_2)$$

$$= \frac{k}{k-1} (P_1V_1 - P_2V_2)$$

$$= \frac{k}{k-1} P_1V_1 \left[1 - \left(\frac{P_2}{P_1}\right)^{\frac{k-1}{k}}\right]$$

(B-15)

from the relationship:

$$PV^k = P_1V_1^k = \text{constant} \qquad \text{(B-16)}$$

where $k = C_p/C_v$.

From the equations (B-12) through (B-15), one can obtain:

$$u_2^2 = u_1^2 + \frac{2g_c k P_1 V_1}{k-1}\left[1 - \left(\frac{P_2}{P_1}\right)^{\frac{k-1}{k}}\right]. \qquad \text{(B-17)}$$

But $u_2 = 0$ for the Pitot tube, and $V_1 = 1/\rho_1$, then Equation (B-17) becomes:

$$u_1 = \sqrt{\frac{2g_c P_1 k}{(k-1)\rho_1}\left[\left(\frac{P_2}{P_1}\right)^{\frac{k-1}{k}} - 1\right]}. \qquad \text{(B-18)}$$

For the steam $k = 1.305$* and adding the friction coefficient to Equation (B-18):

$$u_1 = C_o\sqrt{\frac{2g_c k}{k-1}}\sqrt{\frac{P_1}{\rho_1}\left[\left(\frac{P_2}{P_1}\right)^{\frac{k-1}{k}} - 1\right]}$$

or $$u_1 = C_1\sqrt{\frac{P_1}{\rho_1}\left[\left(\frac{P_2}{P_1}\right)^{0.234} - 1\right]} \qquad \text{(B-19)}$$

where, $$C_1 = C_o\sqrt{\frac{2g_c k}{k-1}}$$

---

* arbitrarily chosen; k= 1.3 with Smith, J.M. and Van Ness, H.C., Introduction to Chemical Engineering Thermodynamics, McGraw-Hill Book Co., New York, (1975), Third Edition, p.469, and k=1.329 with Van Wylen, G.J. and Sonntag, R.E., Fundamentals of Classical Thermodynamics, John Wiley and Sons, Inc., New York, (1965), p.600.

To convert the linear velocity, u_1 ft/sec, to mass flow rate, q_i lb/min, Equation (B-19) should be multiplied by

$$(A \text{ ft}^2)(\rho_1 \text{ lb/ft}^3)(60 \text{ sec/min})$$

and becomes

$$q_i = C_2 \sqrt{\rho_1 P_1 \left[\left(\frac{P_2}{P_1}\right)^{0.234} - 1\right]} \qquad \text{(B-20)}$$

where,

$C_2 = (C_o A)(60)\sqrt{\frac{2g_c k}{k-1}}$ (a constant)

P_2 = impact pressure, lb /ft² (or expressed as P_i in some equations)

P_1 = local static pressure, lb /ft² (or expressed as P_s in some equations)

ρ_1 = steam density at P_1, lb/ft³.

Equation (B-20) is a straight line with a slope of C_2 when $\sqrt{\rho_1 P_1 \left[\left(\frac{P_2}{P_1}\right)^{0.234} - 1\right]}$ is taken as the x-coordinate.

A Pitot tube flow meter consisting of 1/4-inch and 1/8-inch tubes for the flow of steam and for the impact pressure tip, respectively, was constructed. The differential pressure between the local and the impact pressures was monitored by a calibrated 25 psid pressure transducer and the voltage drop was recorded on a strip chart recorder. P_1 also was measured by a calibrated 500 psid pressure transducer.

Table B-II presents the experimental calibration

data and these data were plotted in Figure B-2 to determine the slope of the calibration equation.

As shown in Table B-II and Figure B-2, two sets of experiments were conducted; for the first 12 runs steam was passed through the core and condensed to measure the actual flow rate, and for the second set steam was bypassed before entering into the core, condensed and collected in a graduated cylinder for the measurement of flow rate.

Both equations, which were obtained on the basis of the two different sets of measurement, were tested to predict the flow rate of steam. Even though the straight line obtained from the set of measurements for the first group does not pass the origin of the x-y graph in the calibration figure, it was found that the equation obtained from the first set of data had better agreement with the actual flow rate of steam which was determined by the Standard Method mentioned earlier.

Table B-III presents a comparison of the various calculation techniques for the measurement of steam injection rate into the core. As shown in that table, the weighing method was the most reliable one and the simplest one as well. The power-rating and Pitot-tube methods had some occasional large deviations, indicating that a careful experimental technique is needed: however, in general, these methods still are in

good agreement.

TABLE B-II

Calibration Data for the Pitot Tube Flow Meter

Run	P_s, psia	ΔP^+, psid	W, gm	t, min.	q^*, lb/min	x^{**}
Set 1; steam passed through the core						
1	293	5.63	1940	7.57	0.565	0.917
2	298	4.11	2000	9.16	0.481	0.788
3	165	5.35	2000	11.00	0.399	0.675
4	166	4.64	977	6.33	0.340	0.631
5	168	1.87	1000	11.00	0.200	0.404
6	110	3.56	1000	8.55	0.257	0.454
7	113	2.27	1490	17.50	0.187	0.368
8	114	0.767	502	12.80	0.086	0.215
9	115	0.370	78	8.28	0.0207	0.150
10	114	0.387	190	7.62	0.0549	0.153
11	66.5	1.95	648	10.00	0.142	0.263
12	68.5	0.719	220	10.00	0.0485	0.162
Set 2; steam bypassed						
13	64.5	4.32	1520	14.40	0.232	0.383
14	67.5	3.13	1700	19.20	0.196	0.335
15	69.5	1.52	412	6.78	0.133	0.238
16	69.5	0.577	248	6.54	0.0835	0.146
17	112	0.393	400	10.10	0.0873	0.152
18	112	1.02	653	10.00	0.143	0.246
19	111	1.98	890	10.00	0.196	0.341
20	108	3.43	1210	10.00	0.266	0.441
21	106	4.97	1430	10.00	0.316	0.525
22	161	6.33	2000	10.00	0.442	0.725
23	161	4.28	1640	10.00	0.361	0.597
24	163	2.89	1340	10.00	0.295	0.494
25	165	1.64	1000	10.00	0.220	0.375
26	167	0.377	468	10.00	0.103	0.181
27	213	0.400	571	10.00	0.125	0.209
28	211	1.60	1110	10.00	0.245	0.417
29	209	3.35	1630	10.00	0.359	0.600
30	208	4.66	2010	10.20	0.431	0.705

* $q = W/(453.6t)$

** $x = \sqrt{\rho_s P_s \left[\left(\frac{P_i}{P_s}\right)^{0.234} - 1 \right]}$

\+ $\Delta P = P_i - P_s$

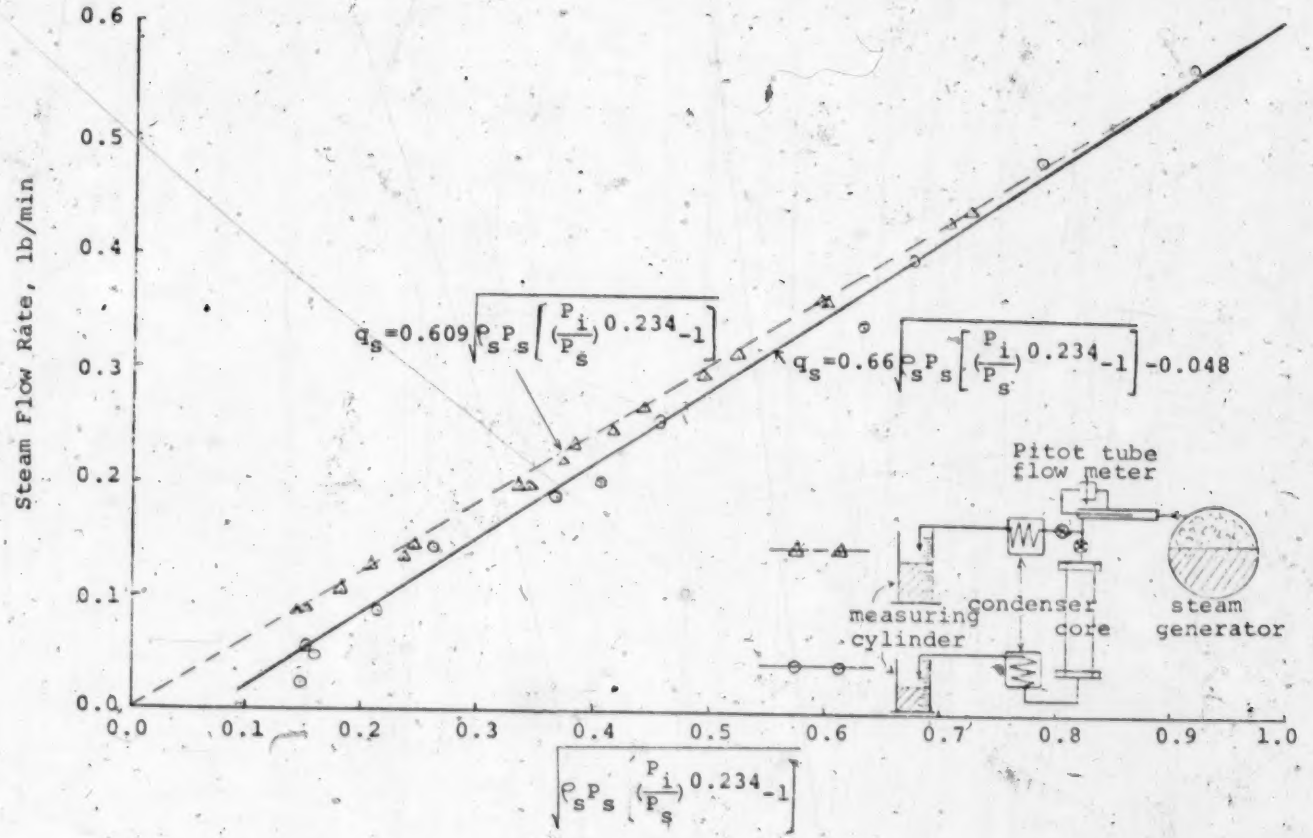

Figure B-2

Calibration of Pitot Tube Flow Meter for Steam Flow Rate Measurement

TABLE B-III

COMPARISON OF VARIOUS CALCULATION TECHNIQUES OF INJECTION RATE OF STEAM

RUN	DATE	STANDARD* (LB/H)	WEIGHING (LB/H)	(PEC.DEV.)	POWER RATING (LB/H)	(PEC.DEV.)	PITOT TUBE (LB/H)	(PEC.DEV.)	PRODUCTION (LB/H)	GPM
1	09/07/76	0.107	0.108	1.6	0.000**	0.0	0.093	-12.9	0.236	1.704
2	17/06/76	0.151	0.146	-3.0	0.000**	0.0	0.138	-8.6	0.360	2.595
3	21/06/76	0.189	0.192	1.3	0.000**	0.0	0.181	-4.3	0.484	3.486
4	23/06/76	0.251	0.225	-10.1	0.000**	0.0	0.222	-11.4	0.604	4.354
5	25/06/76	0.135	0.127	-5.3	0.129	-4.2	0.107	-20.4	0.358	2.578
6	26/06/76	0.156	0.164	4.9	0.156	-0.2	0.156	0.0	0.357	2.577
7	28/06/76	0.169	0.152	-10.2	0.206	21.5	0.195	15.1	0.359	2.587
8	29/06/76	0.133	0.132	-0.2	0.131	-0.9	0.140	5.6	0.358	2.583
9	30/06/76	0.135	0.134	-0.5	0.133	-1.6	0.144	6.2	0.356	2.565
10	02/07/76	0.142	0.141	-0.3	0.144	1.7	0.144	1.7	0.361	2.603
11	03/07/76	0.139	0.139	-0.0	0.140	0.5	0.144	3.5	0.359	2.588
12	05/07/76	0.156	0.154	-1.3	0.158	1.1	0.155	-0.6	0.234	1.688
13	06/07/76	0.200	0.204	1.9	0.213	6.3	0.200	-0.1	0.359	2.586
14	07/07/76	0.233	0.232	-0.2	0.237	2.1	0.230	-0.8	0.485	3.493
15	08/07/76	0.267	0.273	2.0	0.279	4.2	0.262	-2.0	0.612	4.406
16	09/07/76	0.261	0.254	-2.6	0.282	7.8	0.243	-7.1	0.358	2.584
17	10/07/76	0.277	0.299	8.0	0.271	-2.0	0.288	3.8	0.358	2.582
18	11/07/76	0.219	0.226	3.4	0.211	-3.5	0.235	7.5	0.359	2.591
19	23/07/76	0.144	0.144	-0.0	0.119	-17.7	0.142	-1.5	0.235	1.695
20	24/07/76	0.177	0.179	1.4	0.157	-10.9	0.175	-0.8	0.356	2.565
21	25/07/76	0.209	0.222	6.3	0.190	-8.8	0.208	-0.4	0.483	3.480
22	26/07/76	0.254	0.268	5.5	0.000**	0.0	0.205	-19.1	0.627	4.520
23	27/07/76	0.256	0.253	-1.4	0.213	-16.7	0.228	-11.0	0.357	2.571
24	28/07/76	0.296	0.299	1.1	0.270	-8.6	0.280	-5.2	0.356	2.565
25	29/07/76	0.265	0.279	5.2	0.263	-0.8	0.267	0.7	0.355	2.556
26	30/07/76	0.160	0.160	-0.0	0.187	16.6	0.162	0.9	0.232	1.670
27	31/07/76	0.257	0.263	2.4	0.248	-3.1	0.260	1.3	0.481	3.468
28	01/08/76	0.319	0.322	1.0	0.342	7.2	0.318	-0.4	0.607	4.370
29	02/08/76	0.207	0.210	1.1	0.209	0.9	0.202	-2.8	0.356	2.565
30	03/08/76	0.217	0.219	1.1	0.220	1.6	0.217	0.2	0.355	2.560
31	04/08/76	0.158	0.173	9.6	0.155	-1.7	0.166	4.8	0.355	2.561
32	05/08/76	0.160	0.165	2.8	0.149	-6.9	0.159	-0.8	0.356	2.565
33	06/08/76	0.147	0.154	4.8	0.127	-13.7	0.142	-3.5	0.355	2.560
34	07/08/76	0.149	0.151	1.2	0.148	-0.6	0.148	-0.4	0.355	2.562
35	08/08/76	0.194	0.198	2.1	0.192	-0.9	0.188	-3.4	0.481	3.465
36	09/08/76	0.185	0.195	5.2	0.186	0.6	0.191	3.0	0.482	3.476
37	10/08/76	0.151	0.151	-0.1	0.139	-7.8	0.149	-1.5	0.229	1.650
38	11/08/76	0.132	0.132	-0.3	0.127	-3.5	0.127	-3.6	0.230	1.659
39	12/08/76	0.167	0.172	2.9	0.157	-5.5	0.164	-1.8	0.229	1.652
40	13/08/76	0.155	0.163	5.3	0.150	-3.0	0.154	-0.8	0.204	1.469
41	14/08/76	0.159	0.157	-0.8	0.151	-4.8	0.155	-2.3	0.201	1.450
42	15/08/76	0.385	0.388	0.7	0.382	-0.9	0.379	-1.6	0.658	4.741
43	16/08/76	0.166	0.162	-2.7	0.155	-6.7	0.161	-2.9	0.216	1.560
44	17/08/76	0.283	0.283	-0.1	0.284	0.3	0.266	-5.8	0.368	2.651
45	18/08/76	0.104	0.105	0.8	0.097	-6.6	0.101	-2.1	0.188	1.358
46	19/08/76	0.122	0.121	-1.1	0.119	-2.9	0.115	-5.6	0.192	1.383
47	20/08/76	0.140	0.139	-0.7	0.143	1.8	0.132	-5.6	0.206	1.489
48	21/08/76	0.103	0.103	-0.0	0.097	-6.2	0.097	-5.7	0.130	0.942
49	22/08/76	0.167	0.164	-1.6	0.152	-9.1	0.150	-9.7	0.219	1.578
50	23/08/76	0.171	0.168	-1.2	0.168	-1.4	0.174	1.7	0.204	1.469
51	24/08/76	0.166	0.165	-0.7	0.159	-4.0	0.175	5.2	0.194	1.397

* by the material balance of the core ** not measured